Spring 2003

Microreactor system with immobilized enzyme on polydimethylsiloxane (PDMS) polymers

Zonghuan Lu
Louisiana Tech University

INFORMATION TO USERS

This manuscript has been reproduced from the microfilm master. UMI films the text directly from the original or copy submitted. Thus, some thesis and dissertation copies are in typewriter face, while others may be from any type of computer printer.

The quality of this reproduction is dependent upon the quality of the copy submitted. Broken or indistinct print, colored or poor quality illustrations and photographs, print bleedthrough, substandard margins, and improper alignment can adversely affect reproduction.

In the unlikely event that the author did not send UMI a complete manuscript and there are missing pages, these will be noted. Also, if unauthorized copyright material had to be removed, a note will indicate the deletion.

Oversize materials (e.g., maps, drawings, charts) are reproduced by sectioning the original, beginning at the upper left-hand corner and continuing from left to right in equal sections with small overlaps.

ProQuest Information and Learning
300 North Zeeb Road, Ann Arbor, MI 48106-1346 USA
800-521-0600

UMI®

MICROREACTOR SYSTEM WITH IMMOBILIZED ENZYME ON POLYDIMETHYLSILOXANE (PDMS) POLYMERS

by

Zonghuan Lu, B.S.

A Dissertation Presented in Partial Fulfillment

of the Requirements for the Degree

Doctorate of Philosophy in Engineering

COLLEGE OF ENGINEERING AND SCIENCE

LOUISIANA TECH UNIVERSITY

February 2003

ProQuest Information and Learning Company
300 North Zeeb Road
P.O. Box 1346
Ann Arbor, MI 48106-1346

LOUISIANA TECH UNIVERSITY

THE GRADUATE SCHOOL

February 14, 2003
Date

We hereby recommend that the dissertation prepared under our supervision by ZONGHUAN LU

entitled Microreactor System with Immobilized Enzyme on Polydimethylsiloxane (PDMS) Polymers

be accepted in partial fulfillment of the requirements for the Degree of Doctorate of Philosophy

Supervisor of Dissertation Research

Head of Department

Chemical Engineering
Department

Recommendation concurred in:

Advisory Committee

Approved:
Director of Graduate Studies

Approved:
Dean of the Graduate School

Dean of the College

GS Form 13
(1/00)

ABSTRACT

Microsystems, specifically microreactors, open the gate to new, improved analytical techniques while offering many advantages for a large number of applications in chemical engineering, pharmacy, medicine, and biotechnology. This study explored the feasibility of fabrication of microreactors using polydimethylsiloxane (PDMS) as a support for enzyme immobilization. Urease enzyme was used for catalyzing the conversion of urea to ammonia.

PDMS (polydimethylsiloxane) is a silicone-based elastomeric polymer. Traditional micromanufacturing technology was employed for reactor mold fabrication. The mold was fabricated based on photolithography techniques, and SU-8 photoresist was used to construct reactor structure templates. The resulting silicon-wafer based reactor molds were then used repeatedly to generate PDMS microreactors.

One advantage of using an immobilized enzyme system is that the bio-catalyst is retained within the reactor system and enables high concentrations to be maintained. Two enzyme immobilization methods were explored for use with PDMS microreactor systems. One used CMC (1-cyclohexyl-3-(2-morpholineoeethyl) carbodiimide metho-p-tolunensulfonate) as a crosslinker for covalently binding the enzyme to the PDMS microreactor surface. The other employed directly incorporating the enzyme into the uncured polymer. The latter method provided a higher urease activity and was used for most microreactor studies.

To allow an examination of reactor path length, two different reactor templates were applied for evaluation: straight- and wave-channel microreactors. The reactors were tested with different enzyme loadings, feed flowrates, channel lengths, and different operation enviroments. The wave-channel reactors exhibited considerably high urea conversions at relatively higher flowrates compared with the straight-channel reactors. Urea conversion was about 90% in wave-channel reactor with 0.001 ml/min flowrate and 0.01g/g PDMS urease loading, whereas for straight-channel reactor, it is only about 10% urea conversion.

A mathematical model was developed for the microreactors tested. The predicted results were consistent with the experiment results for the straight-channel reactors with short-channels. For the wave-channel reactors, the model showed large deviation from experimented results. The longer the channel length, the greater the deviation. Several assumptions were considered to account for the deviations: channel structure, ammonium ion inhibition, and reactive surface estimation.

TABLE OF CONTENTS

LIST OF TABLES

LIST OF FIGURES

ACKNOWLEDGEMENTS

I would like to express my great appreciation to my supervisor Dr. Bill B. Elmore for his guidance and motivation through this work. I would also like to acknowledge Dr. Palmer for his kind help on my experimental work. I would like to thank my other committee members, Dr. Hegab, Dr. Lvov, and Dr. Frank Ji for their support and encouragement. I also appreciate Mr. Ji Fang and other IFM staffs for their assistance on my microfabrication work.

Last, but not the least, I would like to thank my wife Fang Zhao for being patient and supportive to my research and dissertation work.

CHAPTER I

INTRODUCTION

Advances in precision engineering techniques (on a nanometer to millimeter scale), originally developed for the electronic industry, have enabled researchers to fabricate and test a variety of microcomponents that perform many of the standard unit operations of interest for chemical systems, such as micro-channel heat exchangers, micro valves and compressors. Out of these, the application of micro-fabrication concepts to chemical reactor technology shows a growing field of research, and has been identified as having a number of potential advantages for chemical process development and operation.

Using these techniques, significant reductions in the size and weight of conventional chemical reactor may be realized, enabling distributed and mobile chemical processing and providing the opportunities for the realization of mass production economies through linear scale-up. They have more safety by eliminating storage and transportation of hazardous and toxic chemicals and reduced potential damage due to accidents. The high surface area to volume ratio enhances the control of heat in reactions. Heat and mass transport limitations slow the reaction rates in conventional reactors but are minimized in the micro-channel reactors, thus enabling the use of novel reactions, processes, and the potential for high capacities (throughputs) per unit hardware volume.

The ability to integrate control, sensor, and many other ancillary facilities offers additional advantages over the current complex, multi-unit pilot plant environment[2].

1.1 Microfabrication

Advances in microfabrication technology offer researchers new options in design and fabrication. The technology uses standard integrated-circuits manufacturing steps such as thin-film deposition, ion implantation, lithography, and etching to machine miniature mechanical devices with feature sizes in the micrometer scale or even less. While this technology is currently used to fabricate sensors and analytical instruments, it also offers the ability to design reactors for other purposes such as chemical production[81].

Most of the microscale components demonstrated to date use photolithographic fabrication techniques that have been an outgrowth of the semiconductor industry. A number of other fabrication techniques are in development, and many different materials and structures can be realized. In this study, PDMS (Polydimethylsiloxane) polymer was used as the microreactor substrate. Conventional photolithography techniques were employed for microreactor mold fabrication.

1.2 Bio-Microreactor

It may be possible that microreactors connected by microfluidic devices could permit a complex synthesis process to be finely controlled, avoiding side reactions and resulting in extraordinarily high selectivity. Microreactors would make it possible to

perform many cost-effective trials by consuming minimal amounts of reactant, and can be used for quick screening-an attractive feature, particularly useful in biotechnology.

A novel application for microreactors in biotechnology would be the conversion and production of biological molecules, such as waste remediation system. Enzymes, commonly found in biological systems, immobilized on the microreactor channels can serve as biological catalysts. In the case of urease, the presence of enzyme will liberate ammonia from urea. Many applications can be explored such as aqueous waste purification, which provides drinking and personal hygiene supplies of water in restricted environments[55]. In this case, enzymes have unique importance; they have high advantage over their inorganic counterpart: high activity, high degree of specificity, and the ability to operate near ambient conditions.

Numerous methods are available to immobilize an enzyme to the support, including entrapment, covalent attachment, and adsorption[32]. Immobilizing enzymes offer improved stability. They are retained in the reactor system and enable high concentration to be maintained. Immobilizing also enables the biocatalyst and product/substrate to be segregated, with the possibility of controlling the biocatalyst micro-environment.

1.3 PDMS (Polydimethylsiloxane) Polymer

Most of the microdevices are fabricated using silicon wafers as substrate, employing various micromanufacturing techniques, but many other materials are receiving considerable attention. One of recent interesting substrates is the polymer polydimethylsiloxane (PDMS), a silicone-based elastomeric material. In PDMS

fabrication, a reusable negative mold is first fabricated on silicon substrate using SU-8 photo-resist and conventional wet photolithography techniques. Then PDMS liquid precursor and a curing agent are mixed and poured on the mold for curing. Finally, the cured PDMS is removed from the mold and the desired device deployed by mounting the PDMS microreactor device in an acrylic holder.

Using PDMS as the substrate for microreactor fabrication has several advantages. First, it can reduce the fabrication time by allowing multiple uses of the prefabricated silicon reactor molds. A researcher can fabricate and test reactors with the same configurations, thus reducing the variability that might be experienced in other fabrication processes. Secondly, PDMS is bio-compatible material. It has been found that PDMS contains a regular configuration of silicon atoms. Silanized surfaces provide ready attachment of linker molecules for enzyme immobilization, increasing the possibility of immobilization enhancement.

1.4 Objectives of Research

This study is mainly focused on designing, fabricating, testing, and modeling of bio microreactor system using PDMS as the substrate material, with immobilized enzyme for bio-catalysis. Previous preliminary work in our laboratory (Cynthia K. Dickey[68]) has been done on PDMS reaction system for urea hydrolysis by urease. The chemical reactor was successfully miniaturized to the microscale using PDMS and microfabricating techniques. Enzyme immobilization was achieved by various methods.

However, further assessment of fabrication and performance issues remain: first, the variability between reactors with identical design parameters was high, and this

problem should be studied in detail. Since the conversion is low, new designs should be studied to increase the conversion. Second, experiments showed that the activity of the immobilized enzyme was low, prompting the need to recheck the methods and explore new techniques for immobilization. Third, the former study showed that the diffusion-based model might not be appropriate for reactions catalyzed by biological enzymes on the microscale[68]. By evaluation and modification, further efforts may improve the mathematical model.

While continuing to concentrate on the urea-urease reaction system as a "proof of concept" study, the objectives of this project were as follows:

1. Modify the design parameters of the prototype microreactors to improve the reactant conversion;
2. Explore the enzyme immobilization technology, evaluating the suitable immobilization methods;
3. Analyze the factors which affect activity and stability of the immobilized enzyme in the microreactor system;
4. Evaluate the effect of design parameters (e.g. channel length) and operating parameters (e.g. flow rate) on microreactor performance;
5. Build mathematical model, evaluate the predictions of the model to real microreactors.

CHAPTER II

BACKGROUND

2.1 Microreactor Systems

2.1.1 General Information

Microsystems for chemical applications, specifically microreactors, open the gate to new analytical chemistry and processing techniques, offering potential advantages for a large number of applications in chemical engineering, pharmacy, medicine, and bio-technology. In recent years, microreaction technology has shown an extremely swift development from the first microreactor components described and tested in the early 1990's to recent systematic investigations of microreaction systems[2] [3]. Figure 2.1 shows a comparison of the characteristics for conventional and microreactors.

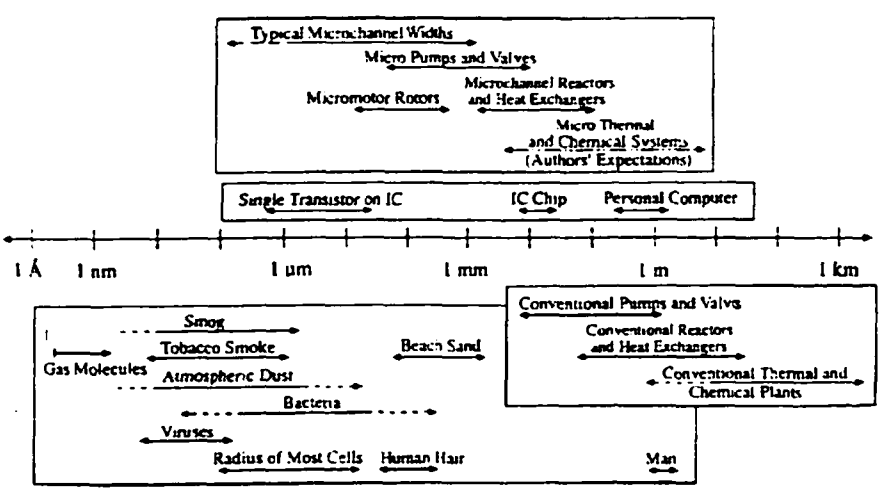

Figure 2.1. Size/Characteristics of Microcomponents Comparison[2]

Starting from first ideas and considerations on potential applications, extensive and wide-spread fabrication of microstructures was followed by feasibility tests, industrial applications of microreactors, and even microplants which contain the complete reaction, separation sequences, all unit and recycle loops, and reduction of feed-rate of a laboratory-scale plant to 10-50 ml/h[1].

At present, it is widely accepted that microreactors open access to new process regimes as well as remarkable process improvements in a timely, and cost-effective manner[2]. Microreaction technology has demonstrated significant process improvements when applied to new reaction regimes not accessible in conventional reactors, such as point-of-use production of explosive or toxic chemical on-site and on-demand[3]. Microreactor systems have shown a capacity for selectivity, yields and conversion rates as well as implementation of new pass-ways for specific reactions. Process improvements- in terms of selectivity and yield, due to the favorable mass, and heat transfer, being inherent characteristics of microreactors-have been reported[1]. The enormous success of combinatorial synthesis and high-throughput screening has broadened the field of screening applications from drug discovery to highly parallel testing of catalysts in gas, liquid and multiphase circumstances, and has stimulated interests in shrinking the whole analytical chemistry or biochemistry lab down to the size of chips which have the ability to integrate sensors, valves, and heaters with the reaction channels to gain more safety, versatility, and functionality[77].

Of various microreaction systems being developed, bio-microreactors have been examined with considerable interest. In this field, enzymes have their special importance: the success of most chemical processes depends critically on catalysis. Enzymes which

are structurally complex protein molecules are the bio-chemical equivalent of conventional counterparts: high activity, high selectivity, and the ability to operate near ambient conditions. Recently, most large-scale bio-catalytic processes in the pharmaceutical, food, and chemical industries have depended on the availability of enzymes for heterogeneous catalysis.

2.1.2 Microreactor Materials (PDMS)

Most microdevices that have been demonstrated recently use microfabrication techniques that have been an outgrowth of the semiconductor industry[2]. Thus, many of the devices are fabricated from semiconductive materials like silicon. While silicon wafers are the most commonly used substrate, metal, glass, and several polymers are often used. Dean W. Matson, et al.[3], have developed a method for fabricating all-metal small–scale chemical processing units using a lamination process. The resulting reactor comprised a solid, leak-tight metal device suitable for high temperature application. Ping Wang, et al.[51], fabricated biocatalytic plastics based on polymeric structures of methyl methacrylate, styrene, vinyl acetate, and ethyl vinyl ether. The resulting reactor systems were used for enzyme catalysis.

Other than non-silicon polymers, micro-scale devices have been fabricated using polydimethylsiloxane (PDMS), a silicone-based elastomeric material. It forms a flexible elastomer with excellent dielectric properties, functioning as durable dielectric insulation, as a barrier against environmental contaminants, and as stress-relieving shock and vibration absorbers over a wide temperature and humidity range. In addition, PDMS is resistant to ozone and UV degradation and has good chemical stability. Figure 2.2 shows a molecular structure of PDMS network.

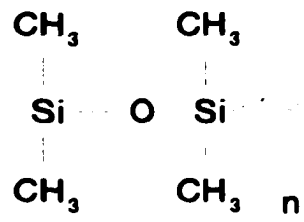

Figure 2.2. PDMS Polymer Molecular Structure

The commercial PDMS most commonly used in microfabrication is Sylgard 184[74] (Dow Corning, Midland, MI) silicone elastomer, which is supplied as a two-part kit comprised of transparent liquid components: base & curing agent. When the base and the curing agent are thoroughly mixed in a 10:1 weight ratio, the medium-viscosity mixture has a consistency resembling SAE No. 40 motor oil, and the hardness of the cured mixture can be adjusted within a certain range by varying the ratio of curing agent to the base. It offers a flexible cure schedule from 25 to 150 °C without an exotherm, and the operation temperature ranges from -55 to +200°C. Sylgard 184 has a specific gravity of 1.05, and has a working time of over 2 hours at room temperature. Its thermal conductivity is about 3.5×10^{-4} °C/cm. After 7 days immersion in water at room temperature, its water absorption is 0.1% (w/w)[74]. The Sylgard 184 silicone elastomer-base & curing agent-will not normally bond to clean, nonporous surfaces, such as metal or glass. A primer coat is required to ensure adhesion to these surfaces. As to the safety issues, the base and curing agent components or their cured mixture do not present any significant toxicological hazard for normal industrial handling.

PDMS is bio-compatible, implantable, and suitable for biological applications (Ratner et al.[68]). Among all bio-medical polymers, PDMS stands out due to a unique property: it self-seals reversibly upon contact with a smooth dry surface, even in a non-clean room environment, probably because the elastomer establishes a high conformal contact with the

opposing surface. Hence, the sealing process is compatible with the presence of thin bio-chemical coatings. PDMS, unlike other polymers that require injection-molding equipment, can be cast inexpensively at air pressure from a thermally curable mixture. A major advantage of PDMS is that multiple (30 or more) devices can be produced rapidly from a single master with only minimal use of clean room facilities. The elastomeric nature of PDMS facilitates the release from the Si mold, as well as other surfaces. After the PDMS replica is peeled off, the mold remains intact and can be subsequently used to create other replicas. PDMS binds moderately to glass and, by extension, to the native SiO_2 on Si. To avoid even partial bonding, which hinders release, the wafers can be pre-coated with 1500 Å of Si_3N_4 in a standard LPCVD (Low-Pressure Chemical Vapor Deposition) furnace or, alternatively, with ~1000 Å of gold in an e-beam evaporator.

A. Folch, et al.[5] explored the feasibility of two technological solutions for creating mold containing deep flat-bottom trenches: photolithography of SOI (Silicon-on-Insulator) wafers and photolithography of SU-8 coated wafers. The first one used Deep Plasma Etch to form the pattern and the mold (master); the second one used SU-8 25 or 50 photoresist to form the molds. To facilitate the removal of the PDMS replica after molding, mold silanization can be used. The master is placed in a desiccator under vacuum for about 1~2 hours with a vial containing a few drops of tridecafluoro-1,1,2,2-tetrahydrooctyl-1-trichlorosilane (United Chemical Technologies, Bristol, PA). A. Folch, et al.[5] found that, for SOI molds, generally, the replication of PDMS structures 20 μm wide (aspect ratio of 2) or wider was flawless; the five-μm-wide structures, due to their high aspect ratio of ~7.5, were unstable and prone to sideway collapse. But the trenches 5-10 μm wide were consistently reproducible. For the SU-8 Mold, they could routinely obtain <15-μm-wide lines or trenches of >50 μm height, but

5~10 μm wide trenches were not successfully replicated. They concluded that PDMS trenches with an aspect ratio of 5 or higher could easily be achieved. This result meets the design requirements of PDMS microchannels for microfluidics applications.

The main benefit of the above methods, apart from the creation of multiple devices by replicating a master, is reusability. The reversible contact of PDMS and other materials allows them to be dismantled and the channel cleaned after use. On the other hand, because it is reversible, the devices may not seal tightly, thereby causing leaking under high pressure. David C. Duffy, et al.[7] introduced the O_2 plasma treatment, and they found that the oxidized surfaces seal tightly and irreversibly when brought into conformal contact. Oxidized PDMS also seals tightly or even irreversibly to other materials used in microfluidic systems, such as glass, silicon, silicon oxide, and oxidized polystyrene. An additional advantage of O_2 plasma treatment is that it yields channels whose walls are negatively charged when in contact with neutral and basic aqueous solutions. They believed that the oxidized PDMS produces a hydrophilic surface with SiOH fragment groups at the surface. The plasma discharge then converts $-OSi(CH_3)_2O-$ groups at the surface to $-O_nSi(OH)_{4-n}$. The formation of bridging, covalent silixone (Si-O-Si) bonds by a condensation reaction between the two PDMS substrates is the most likely explanation for the irreversible seal. Charged PDMS/silicate channels provided two main benefits for microfluidic system over hydrophobic walls: it was easy to fill oxidized PDMS channels with liquids, and the oxidized PDMS channels facilitated molecular attachment. Finally, they found that the oxidized surface degrades quickly if exposed to air; however, it was stable if placed under liquid immediately after oxidation.

The transport behavior of solvents through polymers is important for chemical reaction and separation studies. Such transport properties could figure prominently in biocatalytic reactions, such as our urea-urease system in which the urea could diffuse into the PDMS network to reach the immobilized enzyme. Much research has been conducted in this area for organic vapor sorption in PDMS polymer, which has an extremely good permeation rate, as well as liquid solvents' sorption behavior. C.A. Smolders, et al.[16] studied the liquid and vapor sorption and permeation properties of 14 organics and other materials through PDMS films, ranging from water to chlorinated hydrocarbons. In liquid phase, the permeability ranged cover four orders of magnitude. Similar differences were found in sorption. For example, the sorption of carbon tetrachloride is 0.38g/100g at 40°C. The sorption of the permanent gases is even lower. The sorption increases with increasing number of chlorine atoms or molar volume. In both liquid and vapor phase, it was found that the maximum permeability for chloroform achieved compared with other chloromethanes, suggesting a strong dependency of diffusion coefficients to the solvent activities (concentration). As to the solubility it was shown to increase increases with both activity and molar volume; that is, with the condensability of the solvent. A.G.Andreopoulos, et al.[11] tested the swelling behavior of silicone samples in various solvents at room temperature. The polymer swelling became parabolic with the square root of time, which probably indicated a change in diffusion coefficients of highly swollen specimens. C.J.Guo, et al.[14] studied the effect of molecular size and shape on diffusion of organic solvents in rubbers, and they found that the diffusivity values of methylene, chloride, etc., in silicone rubber, were at least one order of magnitude higher than in natural rubber. The rate of

diffusion of the solvents in both rubbers indicated a clear dependence of diffusion rate on the size and shape of the solvent molecules.

2.1.3 Microreactor Fabrication

Most microreactors are developed through use of microfabrication or micromachining technology. In the narrow sense, microfabrication comprises the use of a set of manufacturing tools based on batch thin and thick film fabrication techniques commonly used in the electronics and semiconductor industry. In a broader sense, microfabrication describes one of many precision engineering disciplines which take advantage of serial direct write technologies, as well as of more traditional precision machining methods, enhanced or modified for creating small three-dimensional structures with dimensions ranging from sub-centimeters to sub-micrometers.

Fabrication techniques include conventional photolithography (mask generation, photoresist coating, pattern transfer, resist striping), x-ray lithography, charged-particle-beam lithography, physical or chemical dry etching using plasma or ion-beam, physical or chemical vapor deposition, epitaxy, bulk or surface micromachining, and the LIGA (*Lithographie, Galvanoformung, und Abformung*) process.

The reactor fabrication involves one or more of the above techniques. Out of them, the most commonly used technique is photolithography. In the integrated circuit industry, pattern transfer from masks onto thin films is accomplished almost exclusively via photolithography. The stencil used to generate a desired pattern in resist-coated wafers over and over again is called a mask. In use, a photo mask, a nearly optically flat glass (transparent to near UV) or quartz plate (transparent to deep UV) with a metal or other

material absorber pattern, is placed into direct contact with the photoresist-coated surface, and the wafer is exposed to the ultraviolet radiation. The absorber pattern on the mask is opaque to UV light, whereas glass or quartz is transparent. A light or dark field image is then transferred to the semiconductor surface.

After resist coating and baking, the resist-coated wafers are transferred to some type of illumination or exposure system where they are aligned; then an exposure system consisting of a UV lamp which illuminates the resist-coated wafer through a mask, thus transfer the mask image onto the resist in the form of a latent image. In photolithography, wavelengths of the light source used range from deep ultraviolet (i.e., 150 to 300nm) to near UV (i.e., 350 to 500nm). In the near UV light, one typically uses the g-line (436nm) or i-line (365nm) of a mercury lamp. The development step transforms the latent resist image formed during UV-light exposure into a real pattern which may serve as a mask for further processing. In this process, the resist-coated wafer was washed with a solvent that preferentially removes the resist areas of high solubility.

Among the various photoresists used in the microfabrication technology, SU-8 (MicroChem Corp., Newton, MA, USA)[75] are used universally especially in the field of MEMS (*Micro Electro Mechanical Structures*). It is a photosensitive negative-imaging resist manufactured for ultra-thick resist applications where high aspect ratio and resistance to harsh etching and plating conditions are required.

SU-8 is an epoxy-based, solvent-developed resist system with excellent sensitivity and high aspect ratio capability. It is based on a photosensitized epoxy resin and a proprietary photo-acid generator which makes hydrofluoric acid upon UV exposure. The reaction cleaves the epoxy groups and creates a cross-linked polyether network, which is

insoluble in the developer solution. SU-8 has light sensitivity in the near UV (350-400 nm), E-beam, and X-ray regions. Its low optical absorption property in the UV region allows one the capability of creating nearly vertical sidewall profiles of features up to 1000 μm thick. Aspect ratios of >20:1 have been achieved. Furthermore, cross-linked SU-8 is chemically resistant when cured above 100°C, and its thermal stability is greater than 200°C. SU-8 will also withstand strong alkaline plating solutions with a pH of 13 at high temperature. Figure 2.3 showed the cross-linked SU-8 photoresist molecular structure. Figure 2.4 showed the relationship of the thickness of SU-8 resist coatings to the spinning speeding of spinner system.

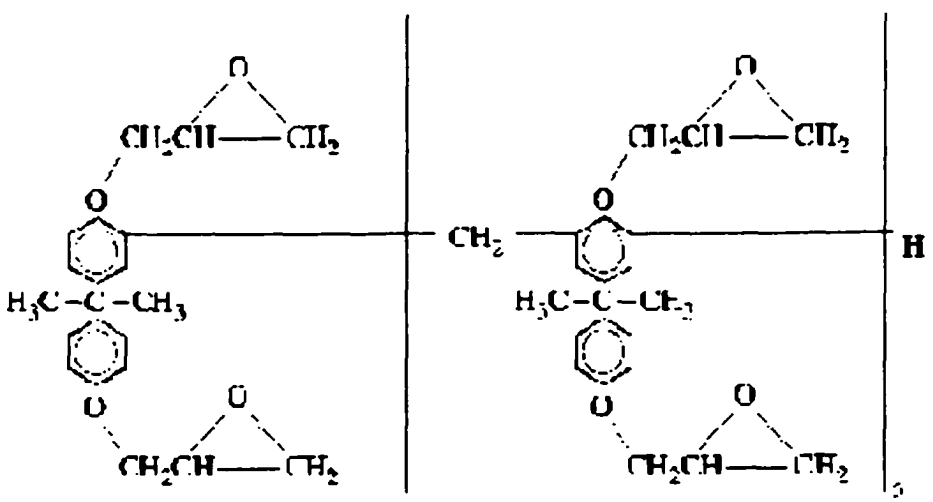

Figure 2.3. Crosslinked SU-8 Photoresist Structure [75]

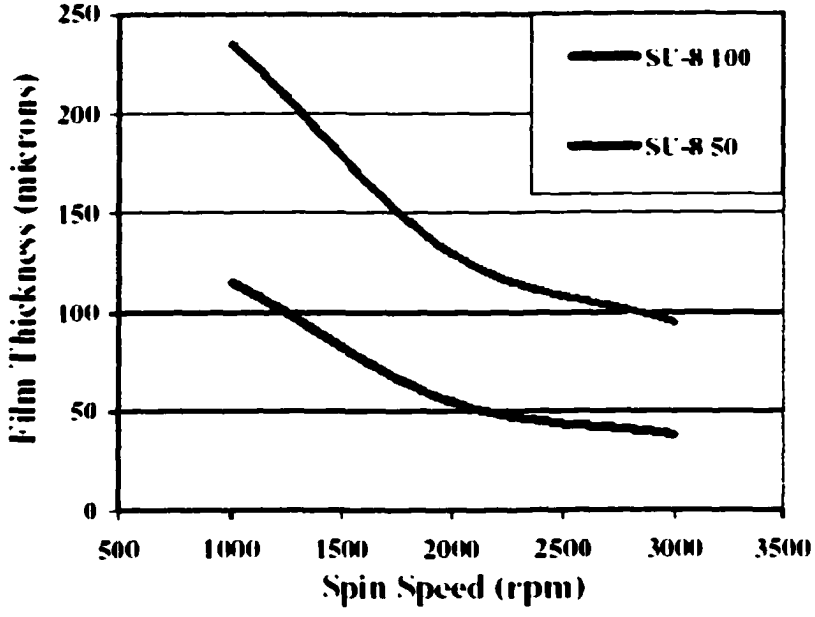

Figure 2.4. SU-8 Film Thicknesses vs. Spin Speed [75]

Due to its high viscosity, the coated SU-8 thickness varies widely depending on the exact coating procedure, including total amount dispensed, spinning time, ramping speed, surface composition, baking time, and temperature, especially for low spinning speed. The SU-8, in contrast to the standard photoresist, is very insensitive to overdevelopment. A. Folch et al.[5] found that projection or proximity photolithography should be used since a ~2mm wide edge bead forms on the edge of the wafer as a result of the surface tension of the coating, which can protrude over the wafer surface by as much as 10 percent of the total layer surface.

2.1.4 Microreactor Dynamics

Similar to conventional reactor dynamics, the microreactor system still involves the fluidics and chemical reaction issues. Microchannels used in the microreactors offer the potential to reduce conventional resistances for mass transport. Single-phase flow in

microchannels is typically laminar (Re < 2000), with heat and mass transport being dominated by diffusion processes. According to diffusion theory, the time-scale (t) necessary to approach complete thermal mixing across the width of a fluid channel (d) is on the order of $t \sim d^2/\alpha$, or $t \sim d^2/D$, where α is the thermal diffusivity of the fluid, and D is the mass diffusivity. Microchannels can reach much less than 1 mm wide, and can therefore be used to construct microreactors that require a very short residence time. A potentially adverse consequence is that realtively large pressure drops will be obtained in fabricated microchannels.

For catalytic reactors, catalysts speed up chemical reaction rates that rapidly reach chemical equilibrium. The catalyst reaction probability is defined as the specific turnover rate to the number of incident reactant molecules. The inverse of reaction probability yields the number of collisions required to form one product molecule. This need for large numbers of collisions emphasizes the advantage of the microreactors with much smaller dimensions over conventional reactors. For enzymes, the reaction activity is defined to characterize the catalytic capability as units of activity per weight or per volume; these units of activity are further defined to catalyze a certain number of moles of reactant per unit time, at specific conditions. Enzyme contains specific regions on their surface known as active sites. When a reactant or substrate contacts the site, a temporary enzyme-reactant complex will form. The reactant will then be transformed by a rearrangement of existing atoms, after which the products of the reaction are released from the enzyme molecule.

2.2 Enzyme Immobilization

Enzyme immobilization is a technique which confines a catalytically active enzyme within a reactor, preventing its entry into the mobile phase so that it can be reused continuously. The use of immobilized enzymes is advantageous in that it retains the biocatalyst within the reactor system enabling high enzyme concentrations to be maintained. It also enables the biocatalyst and product/substrate to be segregated, with the possibility of controlling the biocatalyst microenviroment, leading to enhanced activity while also stabilizing the enzyme. Hence, immobilization can enable prolonged use and so significantly reduce biocatalyst costs, making enzyme immobilization an attractive technique for bio-catalysis.

Some problems do exist with immobilized enzymes. First, like traditional heterogeneous catalysts, they too suffer from the common failing of being rather easily and irreversibly poisoned, often by reactants (substrates) and reaction products. Second, most immobilization does not protect the enzyme from thermal deactivation at temperature exceeding 50°C. Third, although the enzyme catalysis is generally isothermal, the reaction rate expression is normally nonlinear and rather complicated.

2.2.1 General Enzyme Immobilization Techniques

Many methods are available to incorporate an enzyme into a supported matrix, including gel entrapment, microencapsulation, covalent attachment, and adsorption. A wide variety of materials, both natural and synthetic, can be used[29].

Enzyme immobilization via gel entrapment of proteins is commonly employed in biosensor development[28]. This technique has the advantage of being extremely mild,

through amide linkage with primary amines on the protein. Immobilization by adsorption is experimentally simple and can be performed on materials as diverse as steel, titanium, cellulose, and polystyrene. Although not always the case, it is regarded as a mild coupling method that preserves protein activity. However, it can be reversible; moreover, it does not provide as high a surface loading of protein as covalent coupling[28].

Procedures involving covalent binding of enzymes on insoluble polymers have been widely investigated because the enzymes can be very efficiently bound on the support. However, because enzyme activity is sensitive to structural changes, the binding reaction must proceed in such a way that it has as little effect as possible on the enzyme's essential structure. An ideal support material should be insoluble in water but must have some hydrophilic character to provide enzymes a suitable operating environment, and it should be capable of binding enzymes.

Leonard J. Schussel, et al.[40] immobilized alcohol oxidase on a diatomaceous earth support activated using a titanium activation technique with ethylene diamine and glutaraldehyde bridging groups for enzyme linkage. Isabella Moser, et al.[41] studied the capability of immobilizing several kinds of enzymes on metal electrode surface. Different chemical oxidation techniques were applied to activate the highly purified platinum for further derivation. The platinum oxide sites were silanized to obtain amino or mercapto coupling groups. Simon Ekstrom, et al.[42] tested the enzyme immobilization to silicon substrate by three steps, first by silanization in 10% (v/v) aqueous (3-aminopropyl) trithoxysilane, followed by glutaraldehyde activation in 0.1 M sodium phosphate buffer. Finally, the enzyme was coupled in sodium phosphate buffer.

As mentioned at the beginning of this section, polymers are most widely used as substrates for enzyme immobilization. The typical method for enzyme immobilization on polymers is performed by grafting a specific functional group into a performed polymer and modification of side groups of a polymer chain. Jiang Bo, et al.[43] used ultrasonic irradiation to modify polystyrene (PS), which was copolymerized with methyl methacrylate (MMA) and /or glycidyl methacrylate (GMA). The resulting product was used as support for enzyme binding because of the presence of MMA. Anna Wojcik, et al.[45] studied three types of organic polymers and bead-shape silica gels activated by graft polymerization of 2,3-epoxypropyl methacrylate, with epoxide groups for enzyme immobilization. In some cases, the epoxide groups were modified with the addition of NH_3 groups, capable of covalent linkage of amino protein groups by coupling them with glutaraldehyde. The method involves grafting a functional monomer onto the carrier surface capable of enzyme covalent binding. In this case, graft polymerization proceeds with the use of residual double bonds of partially unreacted cross-linking agent molecules in the polymer structure, or by a transfer of the macroradical chain onto the polymer in the process of chain inactivation.

Before copolymerization, silica gel requires prior activation by silanization with a vinyl-silane agent or by the formation of covalently bound radicals which then function as active centers of graft polymerization. The author tested three enzymes: peroxidase, glucoamylase, and urease. The immobilization yield of protein and specific activities of enzymes were better with supports containing NH2 groups than with those containing epoxide spacer arms.

2.2.2 Enzyme Incorporated into Polymers

Most immobilized enzyme applications are performed in aqueous media, and the methods to immobilize enzymes invariably take advantage of the high aqueous solubility of enzymes and the insolubility of polymers. These polymers become critical in providing mechanical integrity, thermal and chemical resistance, and a suitable degree of hydrophobicity/hydrophility, all of which may impact specific advantages in the application of the biocatalyst. Several if not all of these problems can be minimized by incorporating the biocatalyst directly into the polymer matrix during free-radical polymerization. Indeed, this has been used successfully for the inclusion of enzymes into hydrogel materials (e.g., poly [sodium methacrylate] or poly [acrylamide]) where the monomer is highly water soluble[52]. I. A. Kravchenko, et al.[48] also explored proteolytic enzymes immobilized on hydrophilic polymers. Enzymes were embedded into a poly (vinyl alcohol)-poly (ethylene oxide)-glycerol (PVA-PEO-glycerol) gel matrix by directly mixing PVA, PEO, glycerol and proteolytic enzymes phosphate buffer.

Most of the synthetic polymers are hydrophobic. Nearly all vinyl monomers, and particularly those that confer a high degree of mechanical strength, are not water soluble, thereby minimizing the effective interaction between the enzyme and growing polymer matrix. This problem can be overcome, in principle, if the enzyme were soluble in an organic solvent. Ito, et al. have devised a method in which trypsin or pseudomonas lipase could be incorporated into styrenic polymers by attaching an activated enzyme derivative onto the ends of poly (styrene) chains, thereby converting the organic solvent-insoluble enzymes into organic soluble biocatalysts with solubilities of up to 4 mg/ml in

chloroform. Alan J. Russell et. al. also modified two enzymes (subtilisin and thermolysin) with a polyethylene glycol (PEG) which have an acrylate group at one terminus and an active ester at the other terminus, and then incorporated into polyacrylates during free-radical initialed polymerization in a variety of organic solvents. In a flow cell reactor, the biopolymer achieved a half-life of more than 100 days.

Janathan S. Dordick, et al.[47] showed that such organic solvent-soluble enzymes, specifically α-chymotrypsin (CT) and subtilisin, could be incorporated directly in to a variety of plastic-type polymers, from polystyrene to polymethylmethacrylate (PMMA). Not only did the enzyme dissolve, but they also retained their activity in both aqueous and organic solvents. Enzymes contain numerous chemical groups with positive and negative charges, which would cause neighboring proteins to bind together, altering their conformation and hampering their activity, unless these charges were not blocked, or "passivated". Water is well suited to do so, but hydrocarbons in organic solvents can not fulfill this role since they are not polar. Dordick suggests that surfactant molecules can fill in for the water by binding to the positively charged groups on the proteins. The protein is therefore able to resist being forced into an incorrect conformation, and thus the activity of the enzyme tends to be higher. Dordick initially covalently bound enzymes with chemical acryloylation to provide a polymerizable functionality. The modified enzyme is then incorporated into a plastic material via free-radical polymerization of an organic soluble monomer containing an vinyl functionality. Solubilities as high as 20mg/ml were attained for the organic soluble chymotrypsin, thereby offering the potential of achieving high enzyme loadings in plastics. No apparent loss of enzyme was observed in this case.

2.2.3 Stability of Immobilized Enzyme

The lack of long-term stability greatly limits the practical utility of enzymes. Even a "robust" enzyme, such as glucose oxidase is denatured in solution above 55°C, and its half-life at 60°C is only 22 min. Usually in the range of 30 to 50°C, activation of the enzyme prevails and the enzymatic activity increases with temperature, but above that, enzyme denaturation overtakes activation, and the enzymatic activity begins to decline. Increasing enzyme thermo-stability would allow enzymatic reaction to be carried out at higher temperatures; this effect would be help to increase conversion rates and substrates' solubility. It would also help reduce the possibility of microbial growth and the viscosity of the reaction medium. Several strategies have been proposed to enhance enzyme stability: use of soluble additives, protein engineering, chemical modification, and immobilization. In addition to changes in the kinetic parameters of the enzyme reaction, the immobilization step may offer improved stability due to restricted movement of the attached biocatalyst. Joseph Wang, et al.[36] reported on the dramatic enhancement of the thermal stability of several enzymes upon immobilization in carbon paste matrix. Such improvements were illustrated for six enzymes which displayed unusually extended lifetimes upon stressing the corresponding hydrophobic carbon paste biosensors at elevated temperatures (60-80°C) for prolonged periods as long as four months. Gisella M. Zanin, et al.[35] studied the thermal stability of free and immobilized amyloglucosidase in controlled pore silica particles with the silane-glutaraldehyde covalent method. Results showed that free amyloglucosidase maintained its activity practically constant for 240 min and temperatures up to 50°C, but the immobilized enzyme showed higher stability retaining its activity for the same period up to 60°C.

2.3 Urea-Urease Reaction System

2.3.1 Urea-Urease Reaction System

Ureases are hydrolases acting on C-N bonds (nonpeptide) in linear amides. Urease belongs to a group that includes glutaminase, formamidase, and formyltetrahydrofolate deformylase. Urease was first crystallized by Sumner[64] from jack bean meal. The preparative molecular weight of 489,000 appears to be the result of a systematic arrangement of single polypeptide chain subunits of 16x30,000 daltons. Its wavelength of maximum absorbance is 278.5nm, and it activates between pH 4~9. Its isoelectric point is 4.8, and the solubility is extremely small at this pH.

Urea is a highly water soluble, polar non-ionic chemical; hence it is not effectively removed by sorption onto ion exchange media, granular activated carbons, or organic polymer sorbents. Urease-catalyzed hydrolysis is the most efficient way to remove urea from aqueous environments.

The enzyme commission catalog (EC 3.5.1.5) lists the urease reaction as

$$(H_2N)_2CO + 2H_2O \rightarrow CO_2 + 2NH_3 \qquad (2.1)$$

Because two C-H bonds are broken, it is evident that the stoichiometric relation above is the result of two component reactions. The work of Gorin and Blakeley et al.[66] provided convincing evidence that carbamate is the intermediate in a two-step reaction:

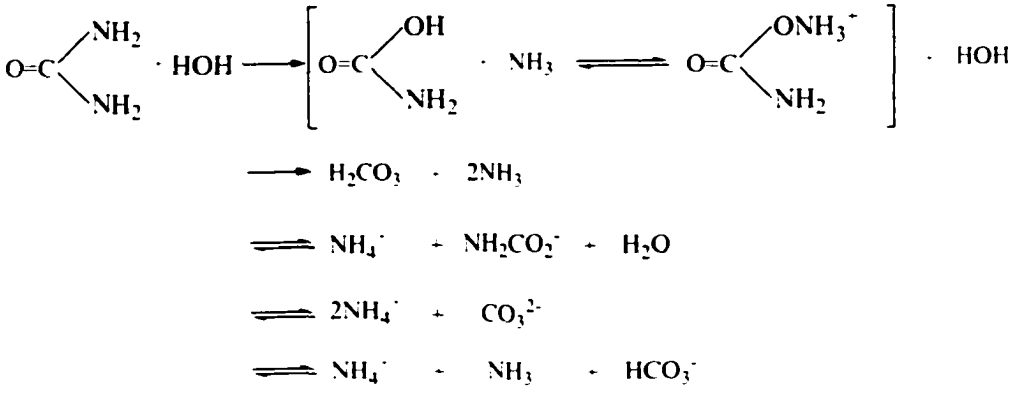

(2.2)

Presumably urease forms a carbamoyl complex

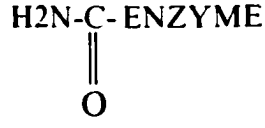

as one of the enzyme-substrate complexes and presumably water is the acceptor in a carbamoyl transfer reaction. Carbamate thus becomes the obligatory substrate for the second step.

Any study concerning the mechanism of the reactions and the nature of the intermediates must encompass the action of inhibitors and the spectrum of substrates. F.J. Reithel[62] reported several organic inhibitors including hydroxamic acids, phenylurea, chlormerodrin, dimethyl sulfoxide. Urease activity persists unaltered when the enzyme is dissolved in 8M urea. Other substrates other than urea like hydroxyurea and dihydroxyurea reversibly inhibited the hydrolysis of urea. The extent of inhibition depended both on the order of addition and the time of exposure of the enzyme to the inhibitor. There is an extensive literature describing effects of various ions on urease activity, indicating the inhibition by copper, zinc, mercury, cobalt, and nickel. The data seemed to indicate that inhibition resulted from the metal substitution of the sulfhydryl group. A phosphate buffer showed some competitive inhibition with urea, as did

ammonia (which was noncompetitive), while trishydroxymethylaminomethane (THAM) and its sulfate provided to be quite satisfactory buffers free from metal ions that neither inhibited nor activated the hydrolysis reaction. The pH of maximal catalytic activity in maleate buffer was 6.5, compared with 7.5 in Tris (THAM) buffer. The rate of hydrolysis at pH 6.9 has been reported higher in potassium phosphate buffers than in sodium phosphate buffer. As to the activators, amino acids such as glycine, DL-alanine, and L-tyrosine enhanced the enzymatic activity of urease[58].

Related studies provided a basis for speculation concerning the nature of the catalytic site. Preliminary kinetic studies suggest that ammonium and sulfhydryl (H-S) groups are involved in the formation of the EX complex, the binding, and that the histidine ($C_3H_3N_2CH_2CH(NH_2)CO_2H$) group is involved in the reaction of the complex, the catalysis[64]. Second, the correlation of changes in enzyme activity with the titration of essential sulfhydryl groups has led to a postulation of eight active sites per molecule. Third, inhibitor binding studies have led to the conclusion that only two active sites are present per molecule, but there is fair evidence for at least eight active regions per molecule of crystalline enzyme[62].

2.3.2 Urease Immobilization

Urease immobilization is being investigated within a wide range of research as a consequence of its possible multiple applications in the medical and technical fields. As supports, natural and synthetic macromolecular compounds have been used, with immobilizations performed through covalent bonding and microencapsulation. Severian Dumitriu, et al.[56] studied the method of covalently immobilization of urease on carboxymethylcellulose with dicyclohexylcarbodiimide as the activator. The author

studied the influence of enzyme/support ratio, activator/support, duration of immobilization, incubation, temperature, metal ions and organic substances, and pH value. The enzymatic activity reached a value of 61.72 μM_{NH3}/min/g, and the resulted product was very stable with time, with enzymatic activity maintained beyond 85% of the initial value three months after synthesis. P.T. Vasudevan, et al.[66] immobilized urease by coupling glutaraldehyde to the silanized support. To immobilize the enzyme, the glass beads were suspended in 15 ml of 0.1 M THAM-sulfate buffer, pH 7.5, and containing 0.25 g of urease power. The coupling was allowed to proceed for 5hrs with intermediate shaking. The resulted activity of the immobilized enzyme was about 3.4IU/g of support. H.J. Moynihan[65] tested urea hydrolysis by immobilizing enzyme onto ion exchange resins in a fixed-bed reactor with coupling agent 1-cyclohexyl-3-(2-morpholineoeethyl) carbodiimide metho-p-tolunensulfonate (CMC). The urease activity for urease on IRP-64 resin has been shown to be as high as 1000 IU/g, but on XP-64 exhibited an expectedly high initial activity of 5500 IU/g. Leonard J. Schussel, et al.[55] tested several immobilization procedures, including immobilization by adsorption onto ion exchange resins, and covalent linkages to silanized glass. The best performance was obtained by immobilizing urease on Celite R-648 controlled porosity diamaceous earth following titanium (IV) oxide activation, and ethylene diamine crosslinking. Activities of the immobilized enzymes were generally $\geq$ 1,000 EU/g. (an EU produces 1 μ-mol-min^{-1} of NH_3 at 25°C and pH 7). Yuri Lvov, et al.[57] explored the method for ordering immobilized multilayers of urease shells on 470 nm diameter latex cores via layer-by-layer assembly. In this study, urease was layered as a negatively charged layer at pH 8 alternatively with polycations (positively charged particles), or as a positive layer at pH

4.5 for alternation with polyanions (positively charged particles). A catalytic activity of the resulting complex colloids was found to be proportional to the number of urease layers in the latex shell, and no urease leakage from the shell was found.

2.3.3 Urease-Urea Catalysis Mechanism

James B. Summer, et al.[64] first demonstrated the formation of ammonium carbamate as the intermediate product in the urease-catalyzed hydrolysis of urea. Jui H. Wang, et al.[33] examined three possible mechanisms for the reaction. The carbonic acid mechanism and the mechanism of directly forming CO_2 and NH_3 without an intermediate step were ruled out. Only the carbamic acid mechanism proved convincing.

K.J. Laidler and J.P. Hoare[59, 60, 61] proposed the molecular kinetics of the urease-urea system. They found the urease-catalyzed hydrolysis of urea had a number of unusual kinetic features. One of these related to the influence of the urea concentration upon the rate of reaction: as the urea concentration was increased from zero the reaction rate first increased linearly, reaching a maximum, and then decreasing. A second characteristic was the sensitivity of the energy of activation to the oxidation-reduction potential of the reaction system, and under certain circumstances its dependency on the temperature. From the rate-concentration curve, they found that the product (ammonium ions) non-competitively inhibited the reaction. By observing that the rates of enzyme-catalyzed reactions vary by less than the first power of the substrate concentration and generally reach a limiting rate at high concentrations, K.J. Laidler[59] found that Michaelis and Menten's treatment is suitable in this situation. The situation is closely analogous to a simple surface-catalyzed reaction for which the kinetics becomes of zero order when the surface is saturated. An extension of the Michaelis and Menten's treatment is necessary

here since a decreasing rate at high urea concentration is observed. K.J. Laidler proposed a model in which a urea molecule and a water molecule must, for reaction to occur, become adsorbed on neighboring sites on the urease molecule: at high concentrations the urea becomes adsorbed on both sites and the reaction is therefore inhibited. Using the model above, as well as considering the effect of ammonium ions and langmuir adsorption isotherm, Laidler derived the reaction rate expression as follows:

$$v = \frac{k_o K C_e C_u}{(1 + K C_u)^2 (1 + K' I)} \tag{2.3}$$

where $\mathbf{k_o}$ is the rate constant for the decomposition of the intermediate complex;

K is the equilibrium constant for complex formation;

K' is the urea inhibition constant

Ce and **Cu** are respectively the enzyme and urea concentrations;

I is the urea concentration.

The complete rate equation is as follows:

$$-\frac{dx}{dt} = \frac{k'x}{[1 + 2K'(a - x)](1 + Kx)^2} \tag{2.4}$$

where **k'** is equal to k_oKCe;

a is the initial urea concentration.

x is the urea concentration

2.3.4 Kinetics of Immobilized Urease Catalysis

K.B. Ramachandran, et al.[58] studied the effects of immobilization on the kinetics of urease-catalyzed reactions in a packed-column differential reactor. The urease was immobilized on nonporous glass beads by covalent bonding by both diazo and

glutaraldehyde coupling. Ramachandran used the low substrate concentration with common substrate inhibition model:

$$v = \frac{V_{max}}{1 + \frac{K_m}{[U]} + \frac{[U]}{K_I}} \tag{2.5}$$

where [U] is the urea concentration;

V_{max} is the maximum reaction rate at certain enzyme level;

K_m is the Michaelis's constant;

K_I is the substrate inhibition constant.

By removing the external mass transfer limits, and the influence of ammonia ions, the effects of pH, urea concentration and temperature effect were studied. The author concluded that the kinetic properties of immobilized urease were similar to those of the soluble enzyme, and different immobilization methods did not appreciably alter the kinetic properties.

However, it is known that the microenviroment of an immobilized enzyme can be quite different from its native soluble form. The effects of diffusion, support materials, buffer, ionic strength, pH value, and temperature may play significant roles in the intrinsic kinetics of an immobilized and its effectiveness.

P.T. Vasudevan et al.[66] analyzed kinetic parameters in a fixed-bed reactor and CSTR containing urease covalently immobilized on a nonporous support in the absence of diffusion limitations, and using the kinetic mechanism derived from Laidler and Hoare[60]. The deactivation studies showed the behavior of the enzyme in the presence of combined urea and ammonia is complicated because the enzyme appears to be poisoned by urea and ammonia both in its free form and in a form complexed with the substrate.

H. J. Moynihan, et al.[65] further proposed a modified Michaelis-Menten rate expression to describe the pH-dependent, substrate- and product-inhibited kinetics when studying urea hydrolysis by immobilized urease in fixed-bed reactor. The rate of substrate reaction R_{urea} is given as follows:

$$R_{urea} = \frac{V_{max}(PH)C_{urea}}{[K_M(PH) + C_{urea}(1 + \frac{C_{urea}}{K_s})][1 + \frac{C_{ammonium}}{K_I}]} \tag{2.6}$$

Where: K_s and K_I are substrate and product inhibition constants;

$$V_{max}(PH) = \frac{V_m}{1 + \frac{K_{ES1}}{[H^+]} + \frac{[H^+]}{K_{ES2}}} \tag{2.7}$$

$$K_m(PH) = K_m \frac{1 + \frac{K_{E1}}{[H^+]} + \frac{[H^+]}{K_{E2}}}{1 + \frac{K_{ES1}}{[H^+]} + \frac{[H^+]}{K_{ES2}}} \tag{2.8}$$

where $V_{max}(PH)$ is the PH dependent maximum reaction rate;

$K_m(PH)$ is the PH dependent Michaelis-Menton constant;

V_m and K_m are the PH independent maximum reaction rate and Michaelis-Menton constant;

$K_{E.1}$ and $K_{E.2}$ are the ionization equilibrium constant of enzyme;

$K_{ES.1}$ and $K_{ES.2}$ are the ionization equilibrium constant of enzyme-substrate complex.

CHAPTER III

MICROREACTOR DESIGN, FABRICATION AND TEST

3.1 Design Validation

In this study, a PDMS (polydimethylsiloxane) polymer was used as the substrate for bio-microreactor fabrication. As discussed in the reviews section, PDMS forms a soft and flexible elastomer exhibiting excellent dielectric, stress-relieving and vibration absorbing properties over a wide temperature and humidity range with a low thermal expansion coefficient of 310 $mm^{-1}C^{-1}$. In addition, PDMS is resistant to ozone and UV degradation and has good chemical stability. PDMS polymer is also bio-compatible. It has been widely used in the pharmaceutical field for manufacturing implantation substitutes, and medical instruments. It is applicable to use PDMS as the substrate for a bio-microreaction system which uses enzyme as the catalyst. Furthermore, among all bio-compatible polymers, PDMS stands out due to a unique property: it self-seals reversibly upon contact with a smooth dry surface, even in a non-clean room environment, because the elastomer establishes a high conformal contact with the opposing surface. And with oxygen plasma pretreatment, it can even form an oxidized surface which seals tightly and irreversibly when brought into conformal contact. Oxidized PDMS also seals tightly or even irreversibly to other materials used in microfluidic systems, such as glass, silicon, silicon oxide, and

oxidized polystyrene. The above chemical and physical properties result in the conclusion that PDMS meets the material requirements for microreactor fabrication in this study.

The fabrication methods favor the use of PDMS as substrate material as well. The common microchannel fabrication method is employed here: first, a master template containing deep, flat-bottom trenches formed by standard photolithography were created on silicon or SU-8 coated silicon wafers. Liquid PDMS was then poured on the template to form a PDMS microreactor. Microfabrication techniques favor the study of reactors in the microscale in this study. The major advantage is that multiple devices can be produced rapidly from a single reusable master with only minimal use of clean room facilities, resulting in nearly identical reactors easily for repeating experiments. The photolithography processes employed also provide easily repeatable mold fabrication. With different masks used, microreactor molds with different design parameters can be easily produced.

Enzyme immobilization on polymers has been extensively studied by many researchers using a wide variety of techniques, such as encapsulation, covalent bonding, and incorporating. Up to now, few studies exist for enzymes immobilized on the PDMS polymer. We have achieved preliminary results for urease immobilized on the PDMS channel surface for different types of reactors. In this study, two enzyme immobilization strategies were evaluated. Different enzyme concentrations were employed, the activity and stability were studied, and comparisons were made between two immobilization techniques.

3.2 Micro Manufacturing Methods

The reactors studied in this study were fabricated using a mold replication method. First, a reactor mold was fabricated; then numerous PDMS reactors were manufactured

by pouring PDMS into the mold, curing, and peeling off from the mold. The mold fabrication method followed the procedure: mask generation, photoresist spinning and baking, photoresist exposure, and finally wet development.

3.2.1 Micro-Reactor SU-8 Mold Design and Fabrication

The mold fabrication of the bio-microreactor incorporated standard photolithography to transfer the images onto the SU-8 photoresist layer on the silicon wafer. The SU-8 used was SU-8 50 (MicroChem Corp., Newton, MA, USA).

The mask pattern for the photolithographic process was drawn using an IBM compatible PC with IC (integrated circuit) design software: L-Edit version 5.17. The mask was drawn with an internal unit equivalent of 1 micrometer and printed to a file in an *encapsulated postscript* format (EPS) with a print ratio of 356 to 1 to ensure that the design has the same dimensions as the actual mask. The design was then transferred to a high-resolution transparency, with the emulsion side down. This procedure provided masks virtually identical in size to the units chosen in the drawing and in actual reactor size.

In Figure 3.1, two reactor designs are shown. In each, a series of micro-scale channels are connected by an inlet and outlet header. Reaction fluid was fed to and removed from microreactor headers via 1/16" stainless tubing and fittings. The tiny triangle features were designed in microchannels. They were used to both increase the enzyme-reactant contacting area, and enhance the reactant mixing in the microchannel.

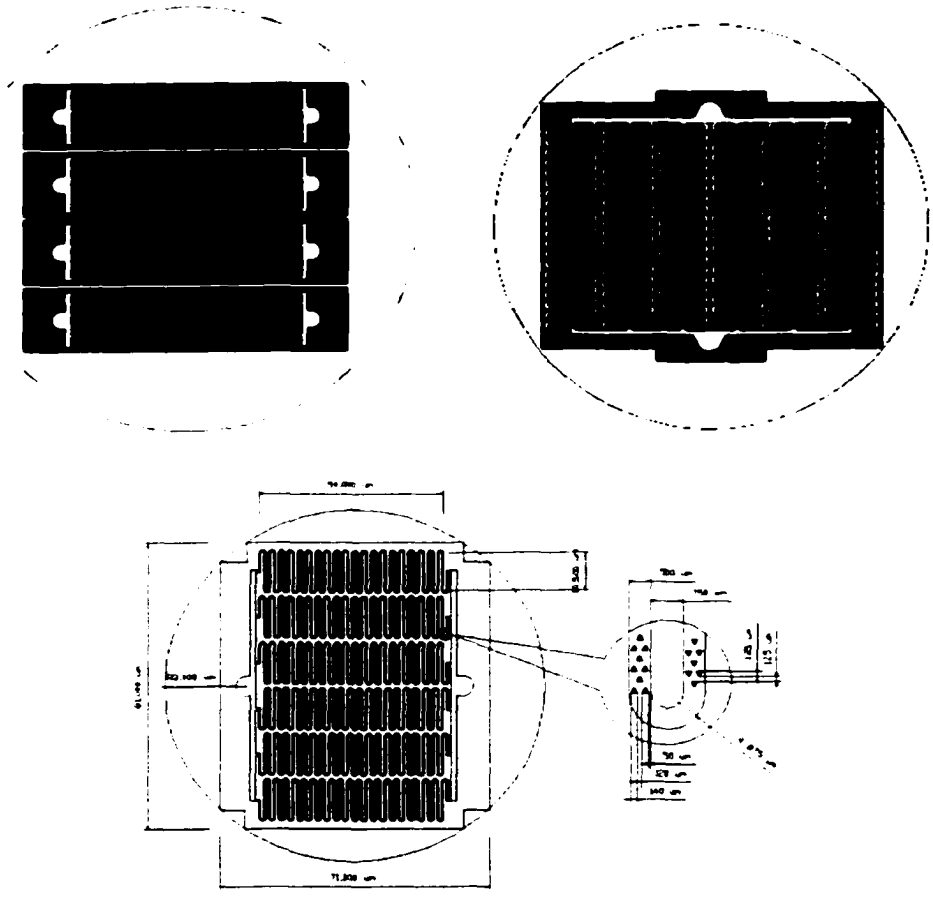

Figure 3.1. Mask Patterns for Microreactors

The mold for the micro-reactors was constructed from SU-8 50 photoresist using a <100> silicon wafer as a support. The fabrication steps were conducted in the cleaning room to avoid SU-8 photoresist coating contamination. The fabrication procedure is described as follows:

1. Wafer Preparation: the silicon wafer was rinsed and cleaned with DI water, acetone, then isopropyl alcohol, and blown dry with anti-static nitrogen. After drying, the wafer was placed on a hot plate (T = 250°C) for 30 minutes for dehydration.

2. SU-8 Photoresist Coating: the wafer was mounted on the vacuum spinning coating system, then a puddle of SU-8 (about 5 ml) was applied and distributed by two spinning cycles (t = 60 sec at 500 rpm each, the resulting thickness was about 200 microns). The spinning speed was adjusted to acquire the desired coating thickness.
3. First Post-Baking Process: following the spinning coating step, the wafer with photoresist was baked for 45-60 minutes at 65 °C in the oven for SU-8 curing. Time by time checking was carried out to ensure no under- or over-curing happened.
4. Mask Pattern Transfer: After the first post-baking step, the wafer with SU-8 coating was mounted on the mask aligner, covered with transparent mask, and exposed to broadband (wavelength is around 460 nm) UV light (24 mw/cm^2) in 1 cycle of 60 seconds. The exposure method is known as proximity printing; the spacing of the mask away from the substrate was about 5 μm.
5. Second Post-Baking Process: after exposing process, the wafer was baked for 15 minutes at 75°C to stabilize the pattern transferred and remove extra solvent.
6. SU-8 Developing Process: the wafer was immersed in the specific SU-8 developer, developed for 16-20 minutes, moving the wafer forth and back as necessary to ensure thorough pattern developing.
7. Post Process: following the pattern developing, the SU-8 mold was rinsed in DI-water to remove the remaining SU-8 developer, and finally blown dry using anti-static nitrogen.

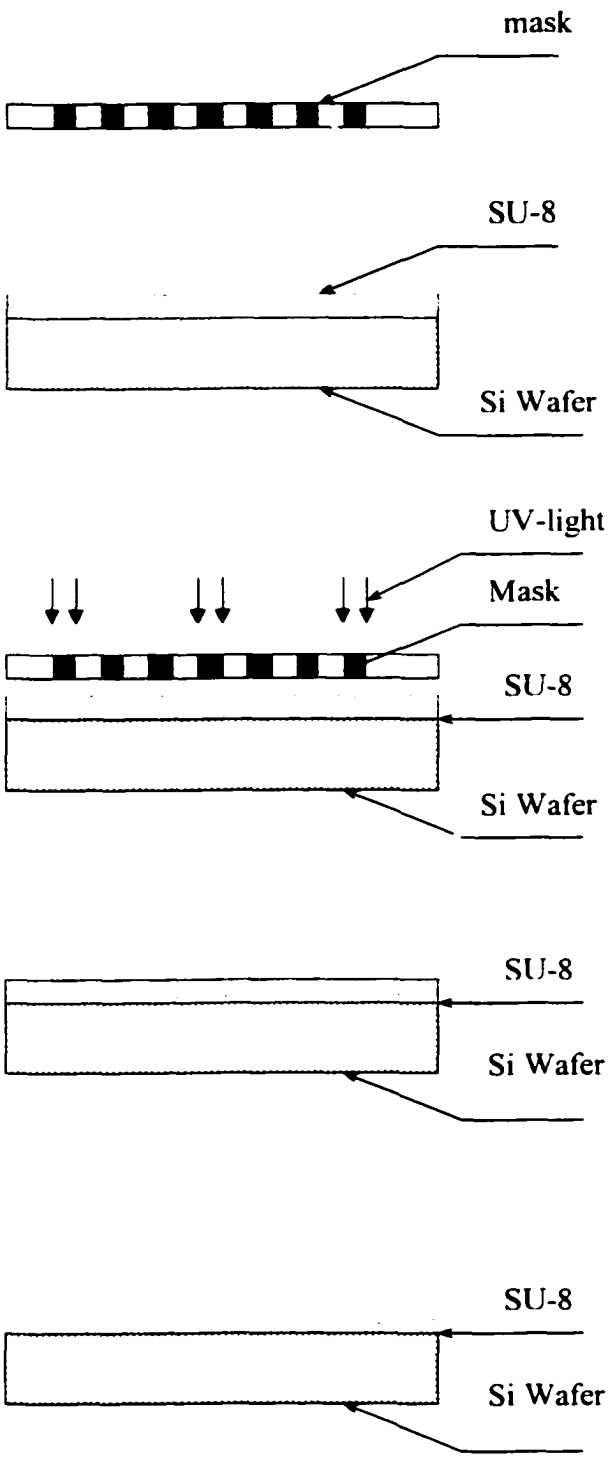

1. Design mask and design transfer to high-resolution transparency
2. Coat a SU-8 layer on the wafer, then bake it on the hotplate for curing;
3. Transfer micro reactor pattern to the SU-8 layer, using mask aligner;
4. Transfer pattern to the SU-8 layer
5. Develop SU-8 photo-resist, remove undeveloped parts, and get the micro-reactor mold;

Figure 3.2. SU-8 Mold Fabrication Procedure

3.2.2 PDMS Reactor Fabrication

Generally, 25g Sylgard 184 (Dow Corning, Midland, MI) silicone elastomer base and curing agent were mixed (10:1) thoroughly and poured on the SU-8/silicon mold, then degassed in the vacuum chamber for one hour and cured on a hotplate (t = 20 min, T = 150 °C) or at room temperature for 72 hours, depending on the enzyme immobilization methods selected. Once the liquid PDMS cured, the PDMS microreactor was peeled off gently from the SU-8 mold.

To reduce the difficulty of separation, the mold can be pretreated by immersing into diluted soap solution for 1 hour and washing thoroughly using DI-water, and drying in the oven at 50 °C. To decrease the leakage probability, another PDMS sheet can be prepared to cover the top side of the reactor due to their self-sealing characteristics. This technique was used only when it appeared necessary.

The produced PDMS reactor was then mounted on the transparent plastic holders, aligned according to the inlet and outlet of the reactor, and tightened by mechanical forces (See Figure 3.3).

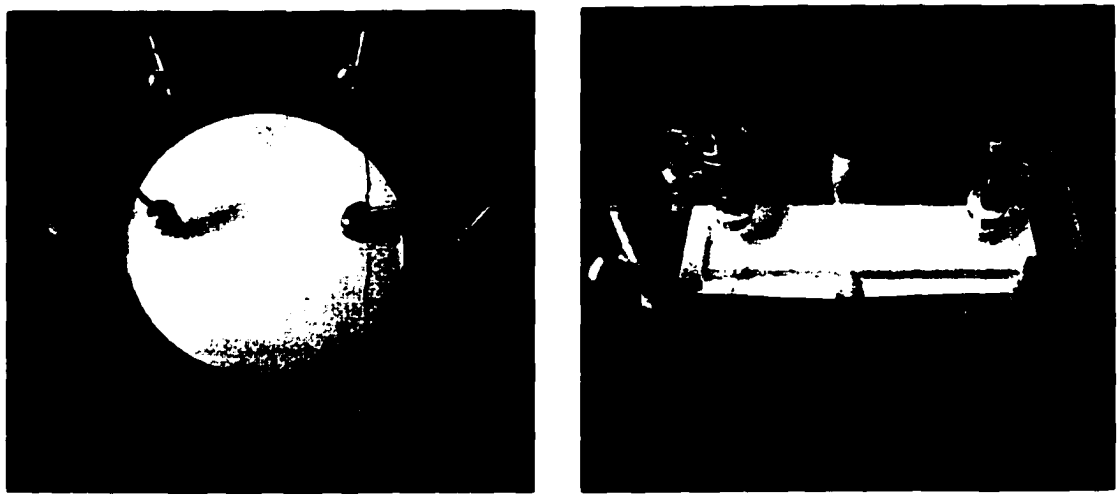

Figure 3.3. Close-ups of PDMS Micro Reactors with Triangle Features

3.3 Enzyme Immobilization Methods

Two enzyme immobilization methods were studied in this research: the covalent bonding method and the direct incorporation method.

The immobilization technique using covalent bonding was described by H.J.Moynihan et al.[65] and Cynthia K. Dickey[68]. The procedure is as follows:

1. Prepare 0.1 M THAM (Tris[hydroxymethyl]aminomethane, $C_4H_{11}NO_3$, FW=121.1, EC No 201-064-4) 100 ml with PH value adjusted to ~7.50 using HCL solution (HCL:H_2O = 1:2 in volume).
2. Dissolve specific weight of urease (CH_4N_2O, FW=60.06, EC No 200-315-5) powder and CMC (1-cyclohexyl-3-[2-morpholineoe-ethyl]carbodiimide metho-p-tolunensulfonate, $C_{14}H_{25}N_3O \cdot C_7H_8SO_3$, FW=423.6, EC No 219-650-3) powder in TMAH buffer solution, stirring at 5°C for 1 hour.
3. Rinse PDMS polymer with THAM buffer (PH ~ 7.50) three times, and then immersed into the solution prepared at step 2.
4. Put the beaker into the refrigerator with continuous stirring at 5°C for 24 hrs for urease immobilizing on the PDMS polymer surface.

Figure 3.4 showed the scheme of urease immobilization on the PDMS surface CMC as crosslinker. The enzyme of urease was covalently bonded to the polymer surface via CMC.

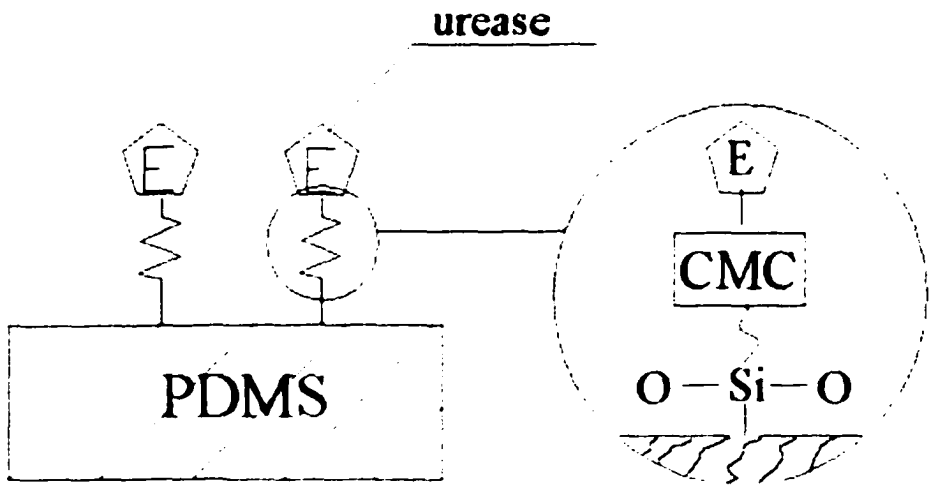

Figure 3.4. Scheme for Enzyme Immobilization by Covalent Bonding

The immobilization technique using direct polymer matrix incorporation before polymer curing is described below:

1. Measure 25.0 g PDMS elastomer (Sylgard 184, Dow Corning) and curing agent together in a 10:1 weight ratio, stirring thoroughly.
2. Measure specific amount of urease power, ranging from 0.1~1.0g, and mix with the prepared PDMS elastomer and curing agent. Stirring thoroughly.
3. Degas in a vacuum chamber for about one hour to remove the bubbles in the mixture. In order to avoid denaturizing of the enzyme, PDMS was cured at room temperature for 72 hours.
4. Keep cured PDMS polymer with immobilized urease in the refrigerator at about 5°C before using.

Figure 3.5 below illustrates the direct incorporation of enzyme into the PDMS. The urease was entrapped or embedded inside the PDMS network.

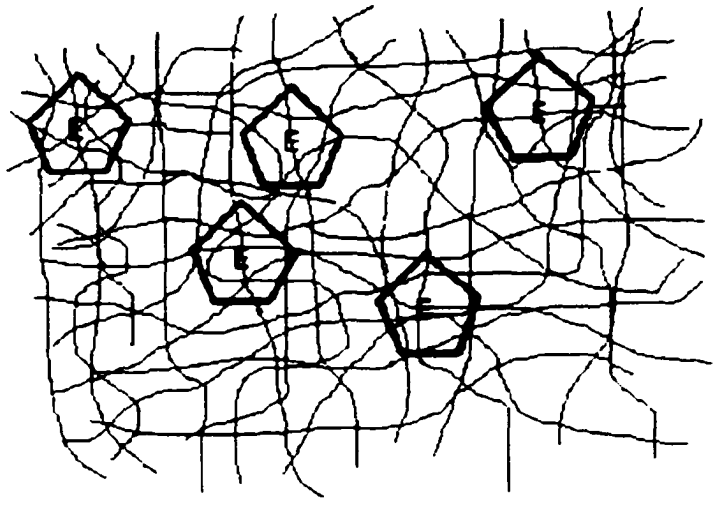

Figure 3.5. Scheme for Enzyme Immobilization by Direct Incorporation

3.4 Analytical Instruments and Methods

In this section two major analytical instruments used in the research were described: an ammonia probe for ammonia measurement and HPLC for urea analysis. The microreactor testing system was also introduced.

3.4.1 Ammonia Detecting by Ammonia Probe

The ammonia electrode uses a hydrophobic gas-permeable membrane to separate the sample solution from the electrode internal solution. Dissolved ammonia in the sample solution diffuses through the membrane until the partial pressure of ammonia is the same on both sides of the membrane. In any given sample, the partial pressure of ammonia will be proportional to its concentration.

Ammonia diffusion through the membrane dissolves in the internal filling solution and to a small extent reacts reversibly with water in the filling solution.

$$NH_3 + H_2O \leftrightarrow NH_4^+ + OH^- \qquad (3.1)$$

The relationship between ammonia, ammonium ion and hydroxide is given by the following expression:

$$\frac{[NH_4^+][OH^-]}{NH_3} = Ka \tag{3.2}$$

The internal filling solution contains ammonium chloride at a sufficiently high level so that the ammonium ion concentration in the internal solution can be considered fixed. Thus,

$$[OH^-] = [NH_3] \bullet Ka \tag{3.3}$$

The potential of the electrode-sensing element with respect to the internal reference element is described by the Nernst equation:

$$E = E_o - Ka \bullet \log[OH^-] \tag{3.4}$$

Because the hydroxide concentration is proportional to the ammonia concentration, electrode response to ammonia is also Nernstian:

$$E = E_o - Ka \bullet \log[NH_3] \tag{3.5}$$

The reference potential, E_o, is partly determined by the internal reference element, which responds to the fixed level of chloride in the internal filling solution, so the electrical potential can precisely reflect the concentration of ammonia.

The method used in this study is for determining the ammonia concentration changes which reflect urea conversion and thus can be used for studying urease activities of both free and immobilized enzymes. By measuring the electrical potential of the sample solution, we can determine the ammonia concentration using a calibration curve prepared according to the tables below.

The ammonia electrode used here is Orion Model 95-10, Cambridge, MA. The calibration curve was constructed using the above tables (note that in all analytical procedure. A pH-adjusting agent [ISA] must be added to all samples and standards immediately before measurement. After addition of the ISA all solutions should fall within a PH 11 to 14 range, and have a total concentration level for dissolved species below 1 M):

3.4.2 Urea Measurement Using HPLC

For reactor testing, the HPLC (High-Performance Liquid Chromatography) was used for measuring urea concentration in the samples. Compared with the ammonia probe method, this method can analyze samples faster and easier, and is suitable for microreactor running tests which require a method to analyze large number of samples in short time, especially for the experiment with several reactors running simultaneously.

In a chromatographic process, species distribute between two immiscible phases in a column: mobile and stationary phase. The rate of migration of each species is determined by the intermolecular interactions such as dipole, ionic, hydrogen bond, and dispersion interactions. Species that mainly distribute into the mobile phase move rapidly. Solute bands grow broader when they pass through the column. As the bands emerge (elute) from the column, their concentration profile, called peaks, are recorded representing the specific species and corresponding quantities.

Three parameters characterize the performance of the HPLC:

1. Retention Factor:

$$K=(T_R-To)/To \tag{3.6}$$

Where $\mathbf{T_R}$ is the time required to elute a peak. **K** is constant for a particular solute and phase system, and depends only on **Kc** (compositions of stationary phase and eluent), **Vm** (the volume of mobile phase) and **Vs** (the volume of stationary phase).

2. Column Efficiency Factor N: it refers to the number of plates generated by a column, and is a measure of the narrowness of the peak. It depends on the size of packing materials, the column length, and mole phase flowrate.

3. Selectivity Factor α:

$$\alpha=K_1/K_2 \tag{3.7}$$

It is the ratio of retention factor of two adjacent peaks, also called capacity factor. It measures the peak spacing, and depends on compositions of stationary phase and eluent.

The objective of chromatography is the separation of mixture components. Resolution is a term defined to quantitatively describe how well this objective is achieved:

$$R_s = \frac{T_{R2} - T_{R1}}{0.5(W_1 + W_2)} = 0.25\sqrt{N}(\alpha - 1)(\frac{K}{K+1}) \tag{3.8}$$

Where W_1 and W_2 is the widths of two adjacent peaks.

The HPLC used here is Hewlett Packard 1100 series. The chromatographic column used is HP Hypersil ODS, a reversed phase column with a dimension of 4.0 x 125 mm. The filling particle size is 5 μm. The mobile phase is dionized water (DI) water with flowrate of 1.0 ~ 2.0 ml/min and pH value of ~6.5, and the maximum signal was detected at 195 nm wavelength for urea via a UV-VIS detector. The HPLC apparatus is shown in Figure 3.6.

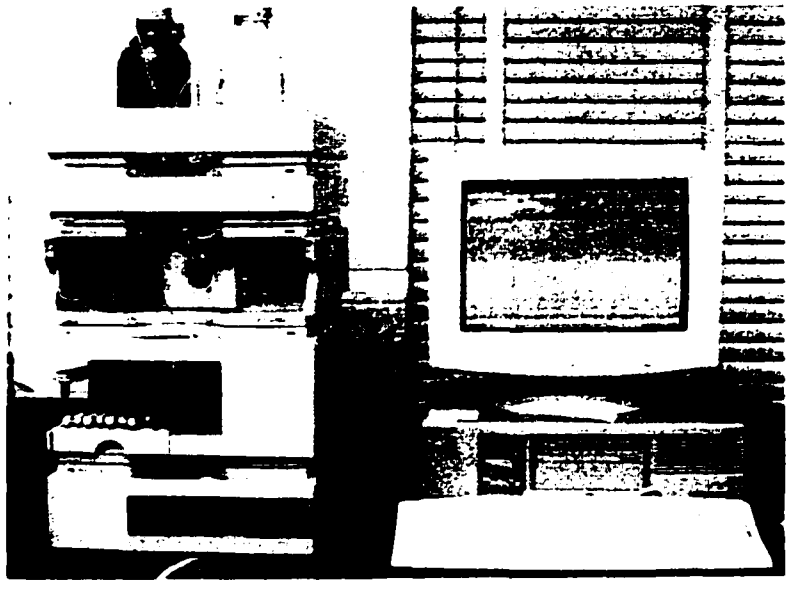

Figure 3.6 Close-up of HP 1100 Series HPLC

While calibration curves were prepared for each reactor run, typical results for urea analysis are shown below in Table 3.1 and Figure 3.7. Linear behaviors observed for all calibrations within our concentration range of interest.

Table 3.1. High level Ammonia Calibration Solution Preparation for HPLC

Step	Added urea solution (0.1M)	Added THAM buffer (0.1 M)	Urea concentration (mol/L))
1	100 ml	0 ml	0.1
2	50 ml	50 ml	0.05
3	10 ml	90 ml	0.01
4	5 ml	95 ml	0.005
5	1 ml	99 ml	0.001
6	0.5 ml	99.5 ml	0.0005

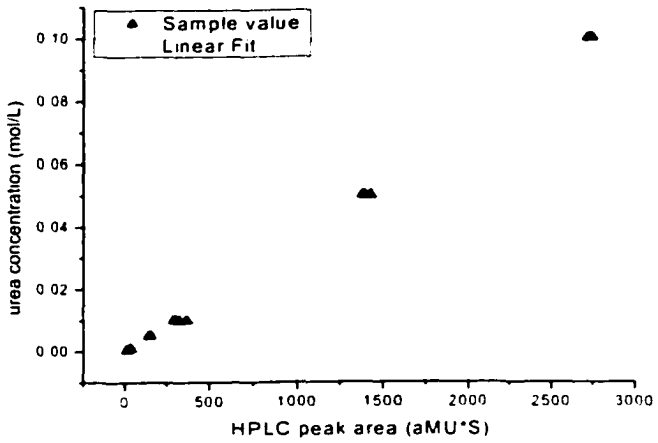

Figure3.7. HPLC Urea Concentration Calibration Curve

3.4.3 Bio-Microreactor Test Assembly

In this study, the microreactor system was set up as shown in Figure 3.8 below; it included a syringe pump (model 74900 series, Cole Parmer), reactors being tested, reactor holders, and testing tubes for sample collection.

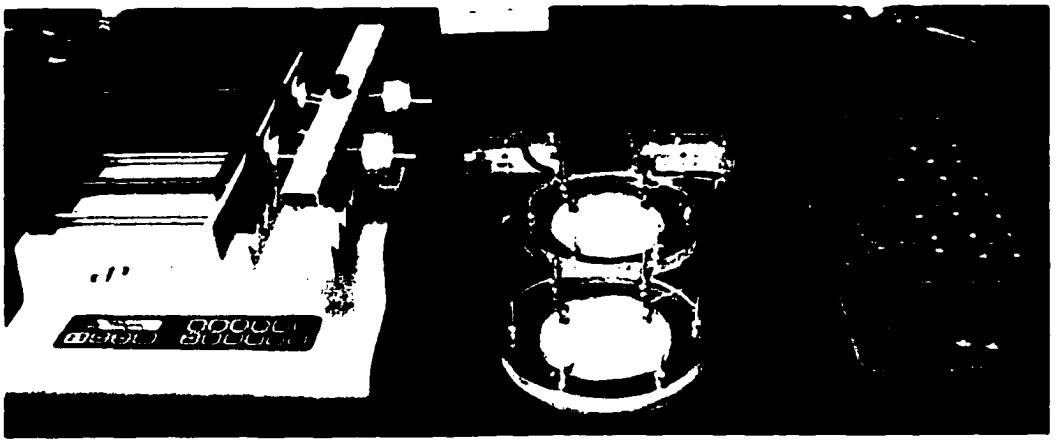

Figure 3.8. Scheme for Bio-microreactor Assembly

The PDMS microreactor with immobilized enzyme was fabricated as the above section described. After sealing the reactor with a PDMS sheet, the reactor was mounted to the transparent acrylic reactor holder. After being aligned carefully according to the

inlet and outlet, the reactor was tightened to prevent leaking. Then the reactor was connected to syringes (vol. 50 ml, dia. 32.75 mm, Hamilton) on the syringe pump. Leakage was tested using DI-water with flowrates equals to the range of actual operating conditions (typically 0.5~1.0 ml/min).

3.5 Analytical Procedure

In this research, effects of the enzymatic activity by immobilization were studied; the microreactors with the immobilized enzyme were tested to evaluate the influence of design parameters and conditions on the immobilized enzyme and reactor performance. The following procedures delineate the processes used for those evaluations.

3.5.1 Urease Activity Analyses

Batch reactor systems (250 ml shake flasks) were used to evaluate urease enzyme activity when attached covalently to PDMS and when directly incorporated into uncured PDMS. The THAM buffer solution was used to control the system pH values. As described in reviews section, THAM buffer neither inhibits nor activates urease activity, thus making it suitable for this study. The pH was adjusted to about 7.4~7.5, the optimum value so that the urease reaches its highest activity.

Procedure for testing urease activity covalently attached to the surface of PDMS is as follows:

1. Prepare 0.1 M THAM Buffer Solution: measure 24.22g THAM solid, dissolve in 100 ml DI-water in a 150ml beaker, then move to a 2L volumetric flask. Add DI-water to the volumetric mark, and stir thoroughly, then seal and store in the refrigerator at 5°C.

2. Prepare PDMS Beads: Mix 50 ml 184 silicon elastomer with 5 ml 184 curing agent in a plastic container, stir thoroughly, move to a cleaned Petri dish (diameter is about 140 mm); then degas in a vacuum chamber for 0.5 hr, finally move into a oven at 70°C for 4 hrs for curing; Then peal off PDMS sheet, cut it into tiny pieces (dimension is W 3mm x L 3 mm x H 3 mm).
3. Immobilize Urease: Measure 100 ml 0.1 M THAM buffer solution, adjust its pH to ~7.40, rinse PDMS beads 3 times using THAM buffer; mix PDMS beads with immobilization solution in a beaker, and put the beaker with stirrer into the refrigerator at 5°C for 24 hrs for urease immobolizing onto the PDMS surface.
4. Prepare the high- and low- level ammonia calibration curve using the 0.1M NH_4^+ standard solution with THAM buffer and ammonia probe.
5. Prepare 0.1M urea solution: Measure 450 ml 0.1 M THAM buffer solution, adjust its pH to ~7.40, measure 2.7027g urea solid, dissolve urea into THAM buffer solution, and measure the PH value and ammonia concentration value.
6. Test Immobilized urease activity: Prepare 3 cleaned 250 ml flasks, take out the PDMS beads with solution from the refrigerator, and remove the urease solution, rinse PDMS beads with 100 ml 0.1M THAM buffer solution (pH ~7.40) three times. Measure total weight of PDMS beads, place in 3 flasks with the same weight for each flask; Distribute 450 ml urea solution into 3 flasks with each flask containing 150 ml urea solution, put flasks on a shaker at 200 rpm, begin the reaction at room temperature. Every 15 minutes take out 2ml sample solution from each flask, and measure the pH value using pH meter (Accumet AR25 PH/mv/Ion/Meter, Fisher Scientific) and ammonia concentration.

Procedure for testing of the activity of urease incorporated and cured with PDMS is as follows:

1. Prepare 0.1 M THAM Buffer Solution: Measure 24.22g THAM solid, dissolve in 100 ml DI-water in a 150ml beaker; then move to a 2L volumetric flask, add DI-water to the 2L mark, swing to mix, and seal and store in the refrigerator at 5°C.
2. Prepare PDMS Beads mixed with urease enzyme powder: Mix 50 ml 184 silicon elastomer with 5 ml 184 curing agent in a plastic container; then measure desired amount of urease powder, also mixed in the same container. Stir thoroughly, move to a cleaned Petri dish (diameter is about 140 mm), then degas in a vacuum chamber for 30 minutes, curing at room temperature for 72 hrs; remove the cured PDMS sheet, cut it into tiny pieces (dimension is W 3mm x L 3 mm x H 3 mm), store in the refrigerator at 5°C.
3. Prepare the high- and low- level ammonia calibration curves using 0.1M NH_4^+ standard solution with THAM buffer and ammonia probe.
4. Prepare 0.1M Urea Solution: Measure 450 ml 0.1 M THAM buffer solution, adjust its pH value to ~7.40 using HCL (2:1 v/v), measure 2.7027g urea solid, dissolve urea into THAM buffer solution, measure the pH value and ammonia concentration value.
5. Urease activity experiment: Prepare 3 cleaned 250 ml flasks, take out the PDMS beads, measure the total weight, put them into 3 flasks with the same weight of 10.00g each, and rinse them with 100 ml 0.1M THAM buffer solution (PH is ~7.50) for three times. Distribute 450 ml urea solution into 3 flasks with each flask containing 150 ml urea solution, put flasks on the shaker with 200 rpm,

begin the reaction at room temperature, and every 10 minutes take out 3ml sample solution from each flask using pipette, measure the pH value and ammonia concentration value using ammonia probe. See Figure 3.9 below for the urease activity experiment setup.

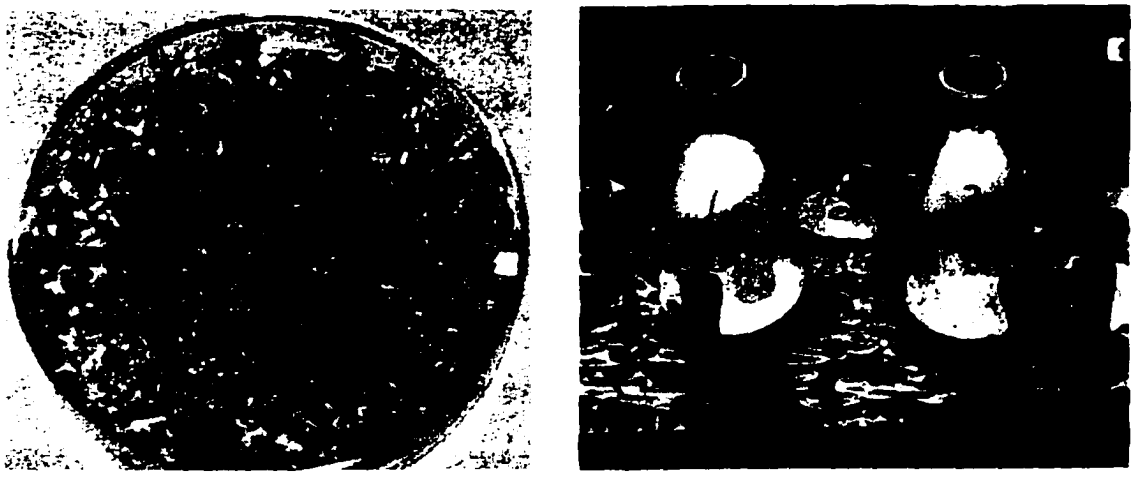

Figure 3.9. PDMS Beads and Immobilized Urease Activity Experiment Setup

3.5.2 Urease Reactor Test Procedure

Experimental procedure for the continuous flow urease microreactor system using HPLC for urea measurements are given as follows:

1. Experiment preparation: first prepare 0.1 M THAM buffer solution by measuring 6.055g THAM solid, dissolving in 500ml DI-water, and adjusting PH value to ~7.50. Then prepare 0.1 M urea solution by measuring 1.5015g urea solid, dissolving in 250 ml THAM buffer solution. Finally fill syringes on the syringe pump with prepared urea solution, each syringe has 50 ml urea solution, begin experiments.
2. Experiment operation: the experiments were operated at varying flowrates of urea solution to evaluate the effects of urea concentration, flowrate, and

enzyme loading level on reactor performance over time. Flowrates were varied in a cyclic manner to access enzyme stability with time. Samples were collected regularly for analysis.

3. Sample Analysis: the HOLC method included, setting the solvent (Dionized Water) to flowrates of 1.0 or 2.0 ml/min, the detector wavelength at 195 nm. A urea calibration curve was prepared for each reactor run. One milliter samples were collected, diluted as needed, and analyzed immediately as obtained. Each sample was analyzed in triplicate, and the readings were averaged.

CHAPTER IV

THEORETICAL MODELING

Reaction kinetics for urea hydrolysis by immobilized urease is presented in this section. Factors influencing the reaction rate are considered, and the substrate and product inhibition on the activity of urease analyzed. A fixed-bed reactor model is applied. The urea concentration profile was determined by combining the mass transport in the reactor channel and the reaction kinetics.

4.1 Urea Hydrolysis Kinetics

The urea hydrolysis reaction by urease catalysis can be expressed as the following expression:

$$(NH_2)_2CO + H_2O \xrightarrow{urease} 2NH_4^+ + HCO_3^- + OH^- \qquad (4.1)$$

The reaction rate for enzymatic reaction obeys a Michaelis-Menten mechanism rate expression. The reaction mechanism consists of adsorption followed by reaction:

$$CO(NH_2)_2 + urease \xleftrightarrow{K_1 | K_{-1}} CO(NH_2)_2 \cdots urease \qquad (4.2)$$

$$CO(NH_2)_2 \cdots urease + H_2O \xrightarrow{K_2} urease + products \qquad (4.3)$$

The local rate of substrate consumption can be expressed in terms of the local substrate concentration, Cs, and enzyme concentration Eo:

$$R_s = \frac{V_{max} C_s}{K_M + C_s} \tag{4.4}$$

where Vmax=K_2Eo,

$$K_M = \frac{(K_{-1} + K_{-2})}{K_{-1}}.$$

The enzyme concentration Eo includes free enzyme, as well as that bound with substrate.

Laidler and Hoare[59] proposed a more accurate extension of Michaelis-Menten kinetics to the urea hydrolysis by urease. The mechanism was based on the formation of a three component reactive intermediate. The reactive complex consisted of the enzyme and two different substrate molecules, urea and water.

$$CO(NH_2)_2 + urease + H_2O \xleftrightarrow{K_1 K_{-1}} CO(NH_2)_2 \cdots urease \cdots H_2O \tag{4.5}$$

$$CO(NH_2)_2 \cdots urease \cdots H_2O \xrightarrow{K_2} urease + products \tag{4.6}$$

The chance of forming ineffective complexes of two substrate molecules with the enzyme increases as the substrate concentration increases, and the reaction rate, in the absence of any other types of inhibition, may be expressed as

$$R_s = \frac{V_{max} C_s}{K_M + C_s (1 + C_s / K_S)} \tag{4.7}$$

Experimental evidence supported the three-component reactive intermediate mechanism as inhibition by substrate and indicated the presence of adjacent active sites on the enzyme molecules.

The parameter V_{max} varies considerably with purity of enzyme and the techniques used for immobilization, both of which affect the concentration of active enzyme. V_{max}

for immobilized urease has been measured as 30% to 60% that of the soluble form used in the preparation. Values have been reported for V_{max} ranging from $6.75x10^{-7}$ (Ramachandran and Perlmetter[58]) to $5.94x10^{-2}$ (Sundaram and Crook[76]) for both soluble and immobilized urease. The Mechaelis-Menton constant for urea have been determined for soluble and various immobilized forms of the enzyme from 3 to 5 mM, while the inhibition constant Ks varies from 3 to 10 mM[58].

The inhibition of urease by the substrate urea has been reported. The substrate inhibition constant is 3.2 mM measured in tris-Maleic acid buffer (Ramachandran and Perlmetter[58]). While substrate inhibition is present in the urease-urea system, it is only manifested at relatively high concentration of the substrate, for less than 100 mM urea, the effects of substrate inhibition can be neglected. In this project, 0.1 mol/L urea solution was used for all the experiments conducted.

The enzymatic hydrolysis of urea is sensitive to product inhibition. Urease is inhibited by the presence of ammonium ions competitively or noncompetitively, depending on the buffer system employed[60].

A competitive inhibitor reacts with the enzyme at the normal substrate binding sites to reversibly form an enzyme-inhibitor complex. Competitive inhibition usually occurs when substances, typically related in structure to the substrate, combine with the enzyme at the same site as the substrate. The competitive inhibitor binds only with the free enzyme:

$$E + I \xleftrightarrow{K_I} E \bullet I \qquad (4.8)$$

Where the enzyme complex EI does not bind with substrate or decompose into products, and K_I is the equilibrium constant for the reaction of the inhibitor with the enzyme. The

effect of a competitive inhibitor is to produce an apparent increase in the parameter K_M by the factor of $(1+C_I/K_I)$. The appropriate kinetic expression for reaction rate becomes (Dixon, and Webb[83]):

$$R_S = \frac{V_{max} C_S}{C_s + K_M (1 + C_I / K_I)} \tag{4.9}$$

Where K_I is the product inhibition constant. C_I is the concentration of ammonia ions.

A noncompetitive inhibitor affects the active site in such a way that the substrate can still be bound, but the rate of reaction is decreased. In this type of inhibition, the inhibitor does not affect the combination of the substrate with the enzyme. Presumably, the inhibitor binds at a locus on the enzyme other than the substrate binding site. The most common type of noncompetitive inhibition is that given by reagents that can combine reversibly with a reactive –SH group on the enzyme molecule, which is essential for the catalytic activity of the enzymes. Such essential groups may be located at the reactive site itself. The noncompetitive inhibitor may bind with the free enzyme, the reactive complex, or both:

$$E + I \xleftrightarrow{K_I} E \bullet I \tag{4.10}$$

$$E \bullet I + S \longleftrightarrow E \bullet I \bullet S \longleftrightarrow E \bullet S + I \tag{4.11}$$

where the ternary enzyme complex EIS does not decompose into products. In each case it has been assumed that combination with substrate does not influence the affinity of the enzyme for another, thus K_M and K_I may be written as the equilibrium constants for the appropriate reactions of the ternary complex. Because of the decrease in reactive complex concentration, the net effect of noncompetitive inhibition is to reduce the parameter V_{max}

by a factor representing the langmuir adsorption isotherm of the inhibitor: $1/(1+C_I/K_I)$. The appropriate kinetic expression for the reaction rate becomes (Dixon, and Webb[83]):

$$R_s = \frac{V_{max} C_s}{(K_M + C_s)(1 + C_I / K_I)} \tag{4.12}$$

The inhibition of urease by ammonia ions has been determined to be noncompetitive in phosphate buffer (Hoare and Laidler[61]), and to be competitive in citrate buffer (Goldstein, et al.[82]). In the THAM buffer system, the inhibition of ammonium ions is determined to be noncompetitive (Vasudevan, et al.[66]). In THAM buffer solution, the value of K_M was reported to be 3.2~5.4 mM, and the value of K_I was 3.0~3.6 mM. (K. B. Ramachandran, and D. D. Perlmutter[58]).

The catalytic activity of urease is known to be sensitive to solution pH value. The soluble urease exhibits maximum activity at a characteristic pH value around 6.5~7.0. The pH dependence of the activity of immobilized urease has been shown to be similar to that of the native free enzyme form. A pH buffer solution is typically used to control the variation of the pH value. In the Tris buffer (THAM) solution chosen for use in this research, the optimum pH value is about 7.4~7.5.

4.2 Governing Equations for Straight-Channel Fixed-bed Reactor

In this study, a straight-channel fixed-bed microreactor model was considered for modeling, and the reaction was considered to homogeneous in the channels and occurring only on the surface of the channel wall and small triangle feature columns. The density of the solution and temperature were taken as constants as well. The concentration distribution of urea within the channel is described by the equation of continuity.

Molar flux rate in	-	molar flux rate out	+	rate of urea formation	= 0	
$W_{Ax}\|_x$	-	$W_{Ax}\|_{x+\Delta x}$	+	$a_c R_A (A\Delta x)$	= 0	(4.13)
$W_{Ay}\|_y$	-	$W_{Ay}\|_{y+\Delta y}$				
$W_{Az}\|_z$	-	$W_{Az}\|_{z+\Delta z}$				

where $\mathbf{a_c}$ = the catalysis surface area per volume of microchannel, and $\mathbf{R_A}$ = overall reaction rate of urea per unit of the catalytic surface area. **A** is the cross section area of the channel. $\mathbf{W_A}$ is the molar flux rate of urea in the channel.

Due to the microscale of the channel in width and depth, the molar flux in the directions of Y and Z can be neglected. Only W_{AX} remained in the equation, which results in:

$$W_{Ax}\big|_x - W_{Ax}\big|_{x+\Delta x} + a_c A \Delta x R_A = 0 \qquad (4.14)$$

Figure 4.1 illustrates the one-dimensional considerations for this model:

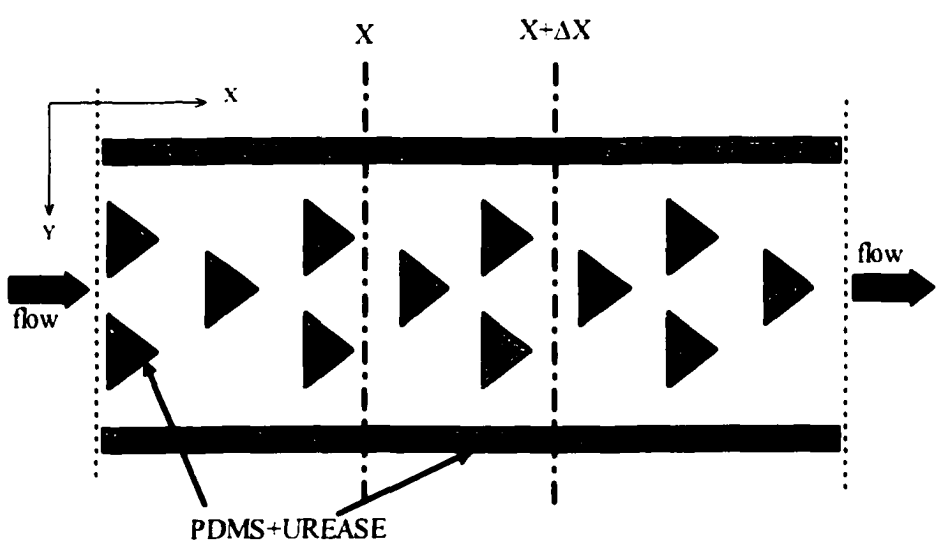

Figure 4.1. Secheme for a Single Straight Microreactor Channel

The molar flux rate of urea in the axial direction of the microchannel is determined by the following equation:

$$W_{Ax} = -D_{AB}\frac{dC_{Ab}}{dx} + y_{Ab}(W_{Ax} + W_{Bx}) \tag{4.15}$$

By neglecting the axial diffusion, the equation reduced to

$$W_{Ax} = y_{Ab}(W_{Ax} + W_{Bx}) = V_x C_t A \tag{4.16}$$

where A is the cross section area of the channel. V_x is the velocity of the solution based on the cross sectional area available for transport. $V_x = G/(\varepsilon A)$, where G is the volumetric flowrate (ml/min), and ε is the fraction of the free cross-section available for transport, which is numerically equal to the fractional void volume.

The overall reaction rate R_A depends on both the rate of diffusion of the urea to the catalytic surface and the reaction kinetics of the catalysts on the surface. In macroscale the diffusion effect usually cannot be neglected, but in microreactor systems, although the flow type is typically laminar flow, the distance that a molecule must diffuse to a surface is greatly reduced. Moreover, the diffusivity for the urea is comparable with the volumetric flowrate: about $1.38\times10^{-5} cm^2/s$, and with the small triangle's mixing effect, the limitation of urea diffusion to the catalytic surface can be neglected. So R_A is only related to the reaction kinetics of urea-urease catalysis on the reactive surface.

For the system with constant density and temperature, substitution of the reaction rate expression and molar flux expression into the above equation of the continuity, results in:

$$V_x A(C_{Ao} - C_A)\Big|_{x,x+\Delta x} - \frac{a_c V_{max}(A\Delta x)C_A}{(K_M + C_A)(1 + C_I/K_I)} = 0 \tag{4.17}$$

where $C_I \approx C_{Io} + 2(C_{Ao} - C_A)\big|_{x+\Delta x}$.

The above two equations are correlated to each other, numerical method is preferred to solve the problems. The first equation can be transformed to the following equations:

$$KC_A^2 - [K(C_{AO} - K_M) - a_c A\Delta V_{max}]C_A - KK_M C_{AO} = 0 \qquad (4.18)$$

where $K = V_r A(1 + \frac{C_I}{K_I})$

$$C_I \approx C_{Io} + 2(C_{Ao} - C_A)\big|_{x+\Delta x}$$

By solving the above equation systems, the urea concentration C_A can be calculated thorough the reactor channels. The final urea conversion could be determined using the above equations once the final urea concentration on the outlet of the reactor was obtained. The values of K_M and K_I can be estimated using the values from literature ((K. B. Ramachandran, and D. D. Perlmutter[58]), the V_{max} and a_c can be estimated via urease activity experiments and measurements conducted.

From the above equations, the influences of the flowrate, enzyme loading, and the reactor channel length on the reactor can be evaluated and predicted. Further the cross-section of the channel has no effect on the urea conversion.

CHAPTER V

RESULTS AND DISCUSSION

5.1 Reactor Fabrication Results

Fabrication of the bio-microreactor in PDMS was achieved by employing standard microfabrication technology normally applied in the IC industry and mold replication method, as presented in section 3. The microfabrication technology was used to generate the reactor molds using a silicon wafer as support substrate and SU-8 photoresist to form the reactor structure mold. And the mold can be used to fabricate many PDMS microreactors by pouring liquid PDMS monomer and curing agent into the mold and peel them off after polymer curing.

The use of silicon/SU-8 for molds generated flat PDMS channels; the depth of the channels is determined by the thickness of the SU-8 structure. In this study, with the photoresist spinning speed at 500 rpm for 120 seconds, the channels yielded uniform depths of about 200 um, and the channel width was 500 um. The triangle features in the channels is about 120 um in both width and height, and the spacing of the features is 160 um.

The spacing of the channels is 750um wide for the wave channels and 1000um for the straight channels. Figure 5.1 provided the SEM (scanning electron microscopy) photos of the SU-8 reactor molds fabricated; the scales used are 1mm and 100 um. As

shown in the photos, the unexposed SU-8 was totally removed from the molds, the channel and feature structures are sharp and clean, no over-etching happened after 16 min development using SU-8 developer.

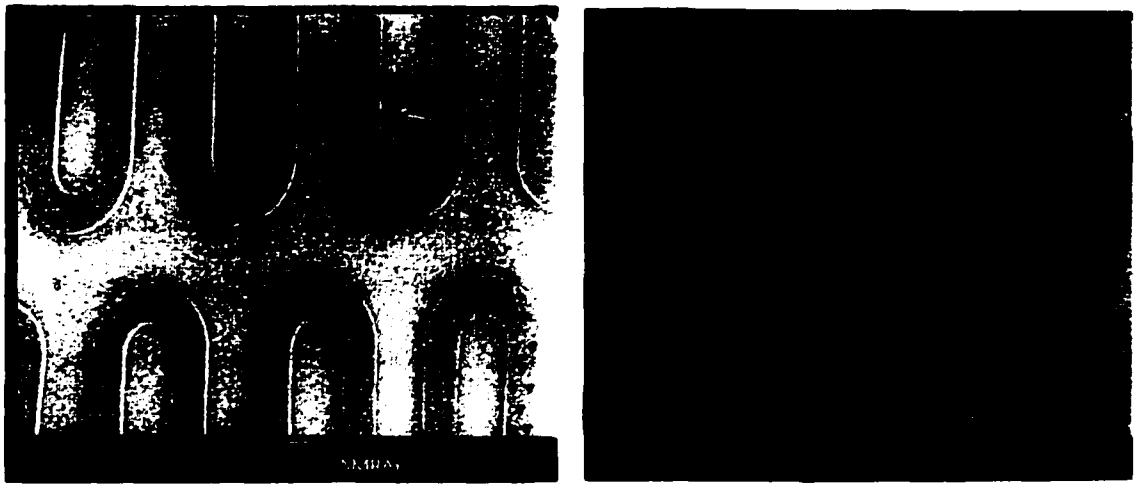

Figure 5.1. Details of Channels with Triangle Features of the Microreactor Mold

Figure 5.2. Close-up of PDMS Microchannels with Triangle Features

The PDMS reactor was peeled off from the mold after curing. The final PDMS reactor channel structure produced are shown in Figure 5.2, with a scale of 100um used, part of channels and one single of triangle feature were examed using SEM. The features fabricated are rather uniform and robust. More than 90% of the triangle features remained

in the PDMS channels after the mold replication procedure. It indicated that the peeling-off process did not affect the final reactor structures too much.

The thickness of the PDMS reactor depends on the amount of PDMS, and the container used, in this study, the resulted reactor thickness is about 5mm. Care was taken to ensure that the container was held level during the curing process.

5.2 Immobilized Urease Activity and Stability Evaluations

Before evaluating the performance of the bio-microreactors, we need to evaluate the enzyme immobilization on the PDMS polymers, its activity, stability, aging, and some other issues. In this study, urease was used as the model enzyme, and the reaction of urea hydro-decomposition by urease was used to evaluate the microreactor system. Two different enzyme immobilization methods were evaluated. The procedures for enzyme immobilization and activity test were described in section 3.3 and 3.5.1. For urease immobilization test, the ammonia probe measured the ammonia concentration changes so as to calculate the urea conversion rate, and a pH meter monitored the pH value changes of the tested solution.

5.2.1 Activity of Immobilized Urease

Before evaluating the activity of immobilized urease, the activity of free enzyme needed to be examined. A 100 ml 0.1 mol/L urea solution (THAM buffered at pH=7.4) was prepared, and 0.06g urease powder (Sigma EC 3.5.1.5) was added to the urea solution. The ammonia concentration and pH value changes were monitored by the ammonia probe and pH meter. The final ammonia concentrations were calculated and

changed to urea converted by immobilized urease. Figure 5.3 showed the urea converted and pH value changing with time.

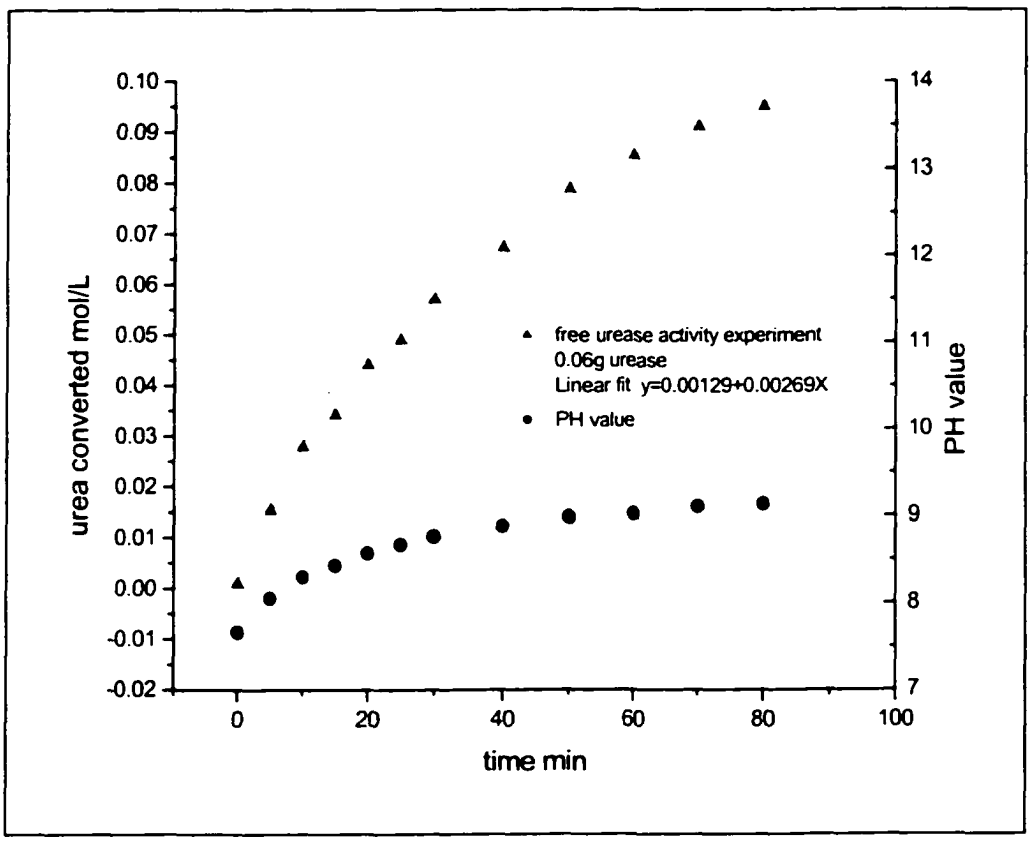

Figure 5.3. Conversion of Urea by Free Urease in Buffer Solution

As indicated in the chart, the urea conversion rate is the fastest at the initial stage but gradually slowed down. In the meantime, the pH value of the solution increased from about 7.5 to the highest of 9.0, which is the upper pH limit that urease maintains its activity without sharp decrease. Illustrated in the plot, the decreased urea conversion rate means the urease began to lose it activity due to the pH increase. The initial reaction rate is 0.00269 M/min, the resulting urease activity is about 44,833 unit/g solid, it is about 67% of the original urease activity, which is 66,700 units/g solid showed on the bottle of the urease purchased.

The activity of immobilized urease on the surface of PDMS by CMC crosslinking method was described in section 3.5.1. In this study, 0.5g urease powder and 0.3g CMC were dissolved in 100 ml 0.1 M THAM buffer solution, (pH ~ 7.4); then about 40 g PDMS beads was added into the solution for 24 hours. After enzyme immobilization, immobilization agent was removed, and the PDMS beads was separated into three beakers evenly, and 0.1 mol/L Urea solution (pH~7.4) was added for enzyme activity test. Figure 5.4 showed the converted urea and pH value changes.

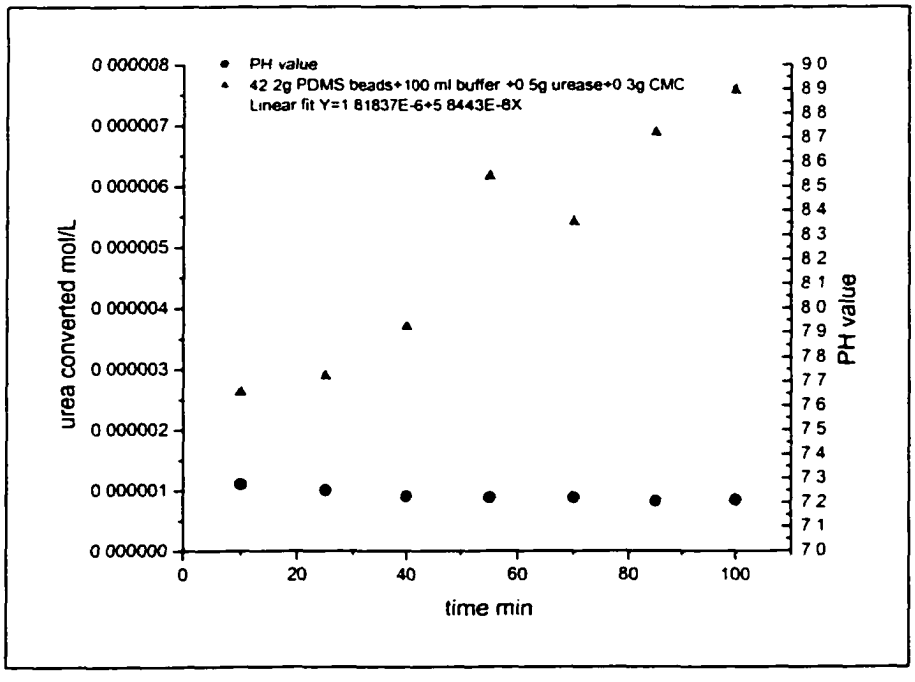

Figure 5.4. Conversion of Urea by Urease Immobilized on PDMS Using CMC

As illustrated in the plot, the pH value of the solution did not change very much. The urea conversion rate is linear, and the conversion rate is very small: 5.8443×10^{-8} M/min. In 100 min, it only converted 1.515×10^{-6} mol urea, and 0.0077% of the total urea in the solution. The result indicated that only a small amount of urease was immobilized on the PDMS surface. Most of the urease still remained in the solution, or

the immobilized urease might lose most activity. Thus it is not suitable to immobilize urease on the PDMS polymer using this method.

The other immobilization method is to directly incorporate urease into a PDMS polymer. In this procedure, urease was directly mixed and cured with PDMS polymer, its activity tests were described in the section 3.3 and 3.5.1. In this study, 0.25, 0.50, and 1.00g of urease powder were directly mixed with 50g PDMS elastomer and curing agent. The resulting bio-PDMS polymer was added into 0.1 mol/L urea solution, (THAM buffered at pH~7.4). The ammonia concentration and pH value changes were monitored. After experiments, the ammonia concentrations were converted into urea converted. Figure 5.5 shows that the polymer with highest urease loading achieved the highest urea conversion rate, and its pH value change is the fastest to reach the 9.0 limit, which slowed down the conversion rate. The initial urea conversion rates were extracted from the data collected, and summarized in Table 5.1.

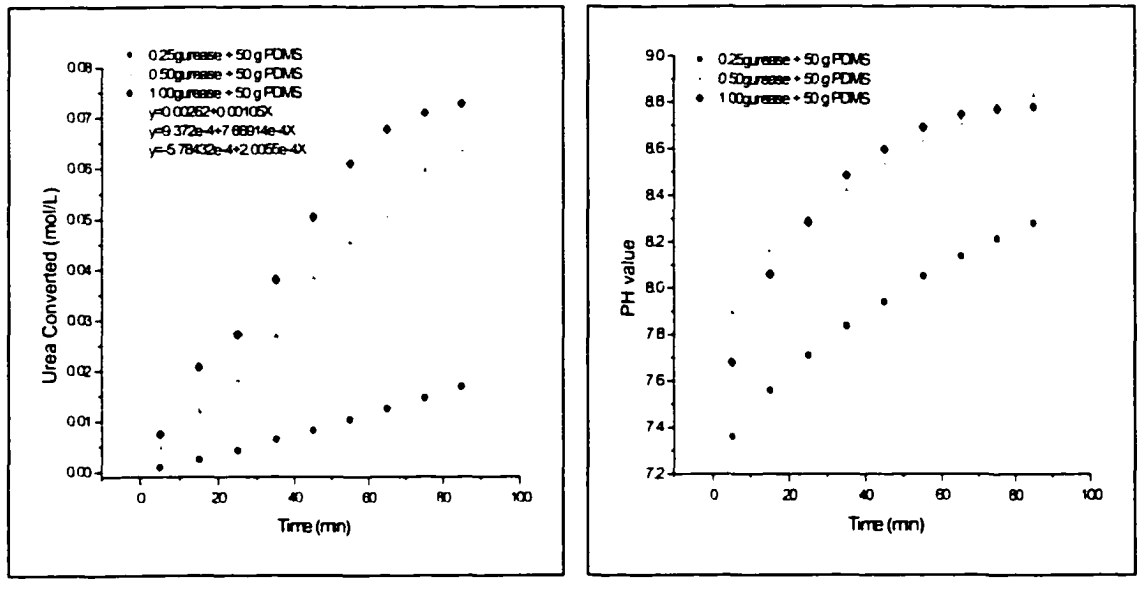

Figure 5.5. Conversion of Urea by Urease Directly Incorporated in PDMS

Figure 5.6 plots the initial urea reaction rate against urease loading in PDMS. The curve on the plot indicates a logarithmic relationship between reaction rate and urease loadings. The more the urease loading, the faster the urea conversion rate, but finally it reached nearly maximum value at about 0.02g/gPDMS urease loading. The maximum conversion rate is about 0.0011M/min.

Table 5.1. Initial Reaction Rates of Urea Decomposition by PDMS Bio-polymer

	Immobilized urease test 1 (0.25g urease + 50 g PDMS)	Immobilized urease test 2 (0.50g urease + 50 g PDMS)	Immobilized urease test 3 (1.0g urease + 50 g PDMS)
Urease loading (g/gPDMS)	0.005	0.01	0.02
Reaction rate (M/min)	2.0055e-4	7.66914e-4	0.00105

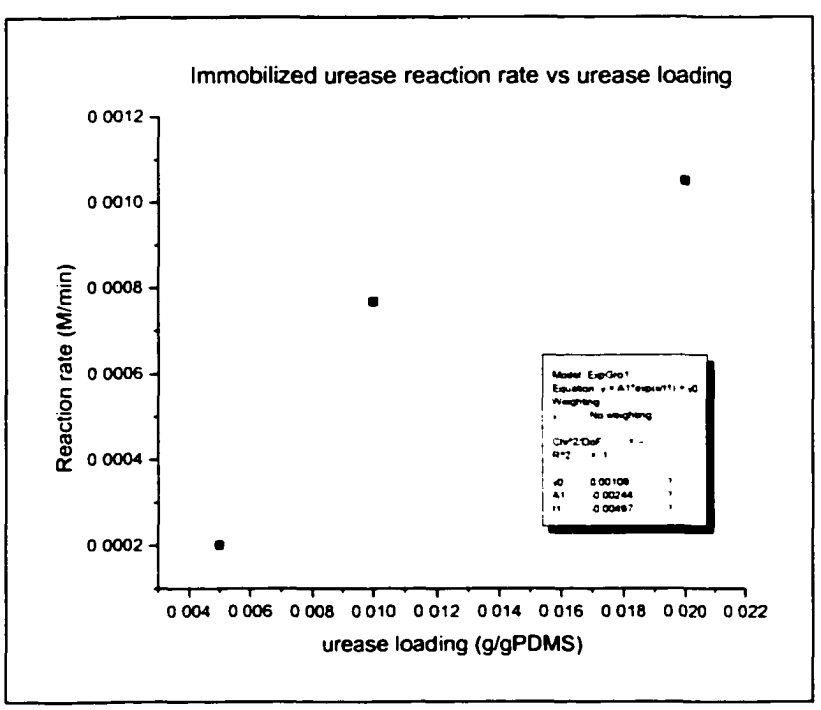

Figure 5.6. Reaction Rate vs Urease Loading for Urease Incorporated into PDMS

5.2.2 Stability of Immobilized Urease

The stability of urease directly incorporated into the PDMS was also tested. 0.25g and 0.50g of urease powder were mixed with 50 g PDMS polymer separately. After curing, the bio-polymers were kept for 30 days before testing their enzymatic activities; the results were compared with the former activity results. Figure 5.7 shows the urea conversion rates against time for the urease incorporated into PDMS after keeping for one month.

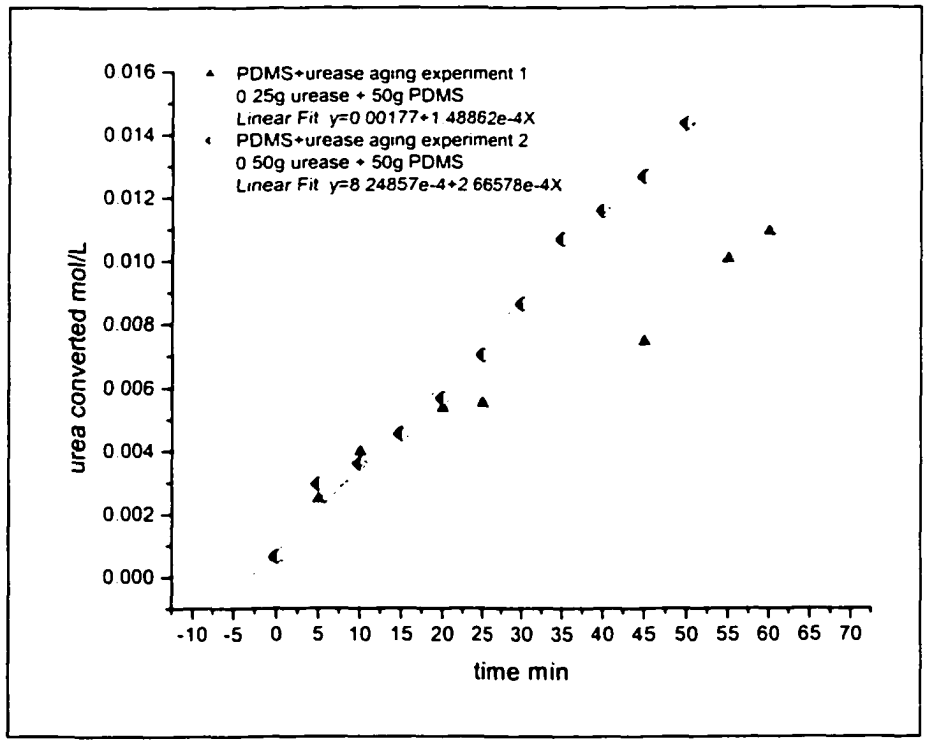

Figure 5.7. Urease-PDMS Polymer Aging Test with Different Urease Loadings

Figure 5.8 compares the urea conversion rates before and after 30-day time intervals. The chart indicated that the urease-PDMS polymer with higher urease loading lost more enzymatic activity than the polymer with lower enzyme loading. In the chart,

bio-polymer with 0.005g/gPDMS urease loading lost about 26% activity, while the polymer with 0.01g/gPDMS urease loading lost 65% activity.

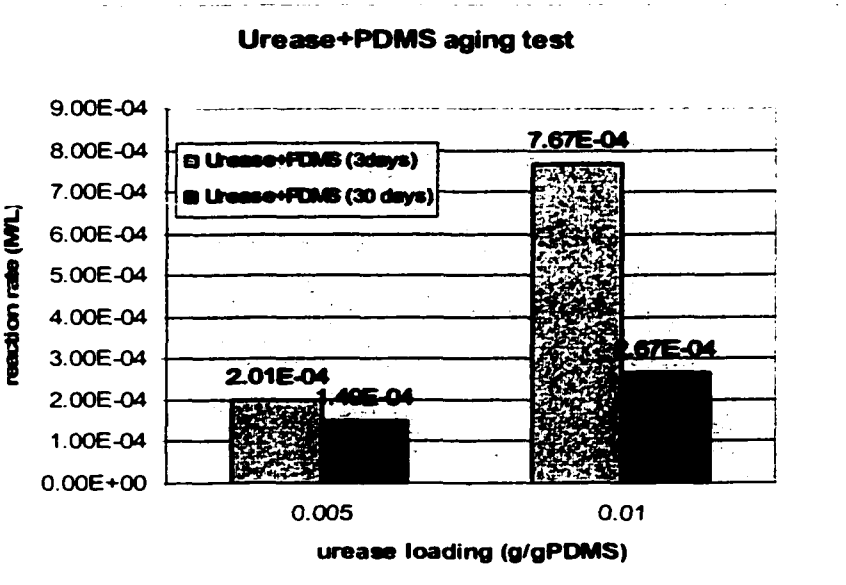

Figure 5.8. Urea Conversion Rates Comparison between One Month Interval

5.2.3 Swelling Property of PDMS Incorporated with Urease

The swelling property of the resulted urease-PDMS polymer has a significant importance. It indicates the polymer's capacity for solvent absorption, and it reflects the polymer's internal structure with incorporated urease. It is important because it can indicate how easily the solvent or reactant can penetrate and diffuse into the polymer and reach the enzyme far from the surface. In this study, PDMS with different urease loadings (0.25 and 0.5g urease with 50g PDMS polymer) were cut into small beads (dimension of W 3mm x L 3 mm x H 3 mm), and immersed into 0.1 mol/L urea solution with THAM buffer at pH~7.4. The weight of the PDMS beads was measured repeatly, the solution was removed from the PDMS polymer surface using filter paper before measurements. The experiments were repeated several times, and the results are shown in Figure 5.9.

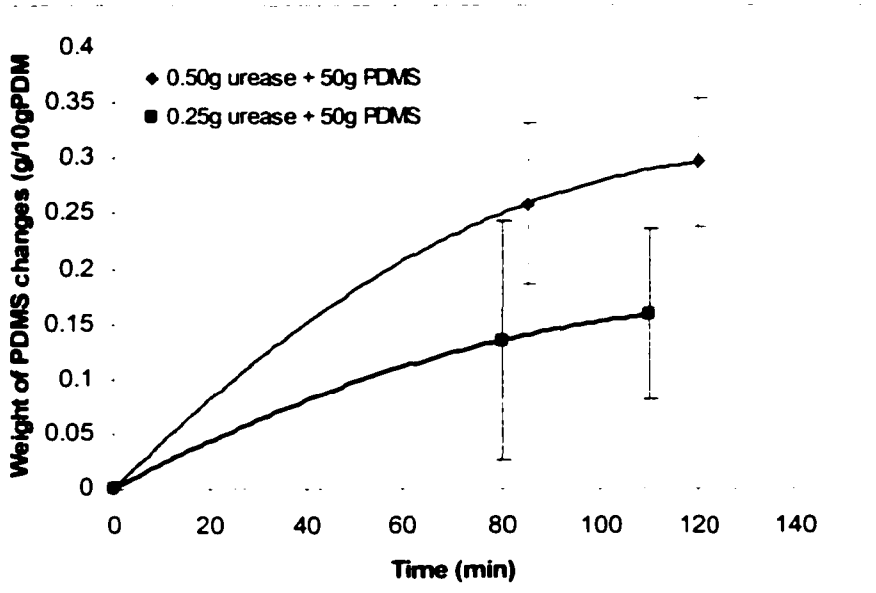

Figure 5.9. Swelling Properties of PDMS with Different Enzyme Loadings

Figure 5.9 indicates that the PDMS polymer with higher enzyme loading adsorbed more solution (increased 3% weight after 120 min immersing in urea solution) than the polymer with lower enzyme loading (increased 1.6% weight after 110 min). Compared with the pure PDMS polymer, which increases only 0.1% weight after 7 days' immersing in water, the results indicates the structure change of the PDMS polymer which allowed solvent easily diffuse into the polymer to reach the immobilized enzyme.

From the above activity tests for immobilized urease with different immobilization methods, and other tests, it is obvious that the activity of urease directly incorporated into the PDMS has much higher than the activity of enzyme immobilized using CMC method. The swelling property of the resulted bio-PDMS polymer also support that it is easy for reactant to diffuse into the polymer and react with urease. Thus for the following bio-microreactor tests, the enzyme incorporation technique was used to immobilize urease to PDMS polymer.

5.3 Bio-Microreactor Performance Evaluations

In this study, three microreactor designs were fabricated, one straight channel design and two wave channel designs. All of them have tiny triangle features in microchannels with specific spacings, the purpose of these small features is to achieve better mixing of reactant in the channel, the tiny features can help to increase reactant mixing state in the channel and let more reactant reach reactive walls, in the meantime, since the features themselves are also reactive, they can help to increase urea conversion. The following table is the types and design parameters of the microreactors tested.

Table 5.2. PDMS Microreactor Design Parameters

	Reactor Description	**Channel Width (μm)**	**Channel Length (mm)**	**Other**
1	Six-straight-channel (with triangle features)	500	50	One inlet and one outlet
2	Six-wavy-channel (with triangle features)	500	500	One inlet and one outlet
3	Two six-wavy-channel in a series (with triangle features)	500	1000	One inlet and one outlet Extended length

The reactors with different designs were evaluated and compared with each other according to the capacities of converting urea into carbon dioxide and ammonia. Also, the reactors with same design but different urease loadings and different reactant feed flowrates were tested to evaluate the influences of different operation parameters on the performance of reactors.

5.3.1 Influences of Buffer and Substrate on the Reactor

Before other parameters of the microreactor were tested, the influence of THAM buffer solution on the reactor performance was evaluated. The microreactor used was six-wave-channel microreactor as described in section 3, the urea concentration at the inlet was 1.0 mol/L, the THAM buffer solution was 0.1 mol/L, and the pH was adjusted to about 7.4 using HCL solution. The reactant was pumped through the reactor by a syringe pump at controlled flowrates. The products were collected at the outlet of the reactor, and the urea concentration was analyzed using HPLC (High Performance Liquid Chromatography), and DI-water (pH=6.5) was used as mobile phase. The signal was detected at 195nm. In this study, the urease loading for the reactor is 0.01g/gPDMS (66,700 unit/g urease powder). Two flowrates (0.023 and 0.06 ml/min) were used.

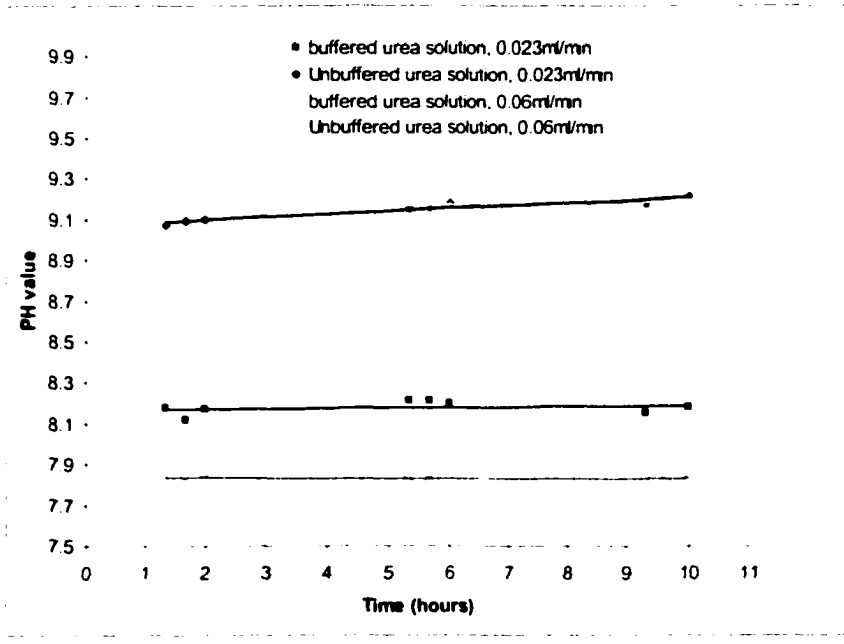

Figure 5.10. PH Changes for Buffer Influence on Reactor Performance

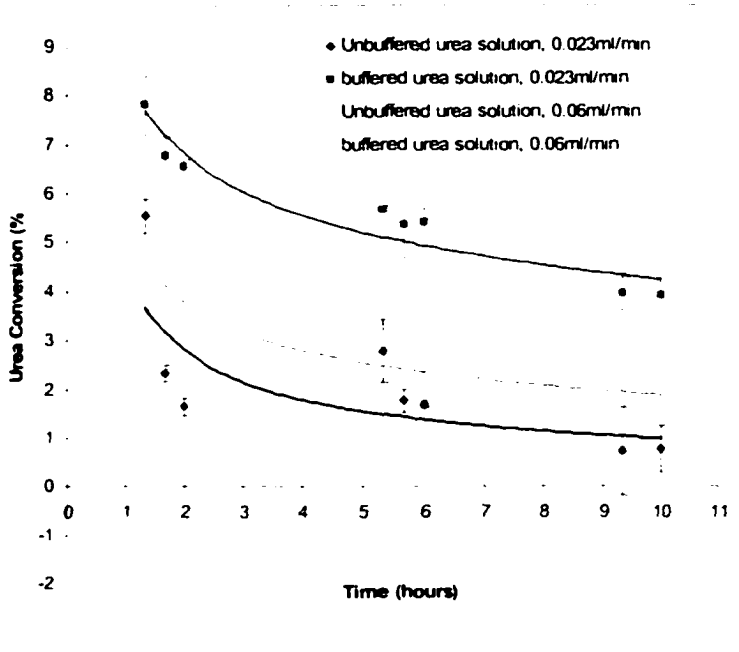

Figure 5.11. Urea Conversion vs Time for Buffer Influence on Reactor Performance

Figure 5.10 shows the pH value changes of the solution at the outlet of the reactor, and Figure 5.11 shows the urea conversion against time at different flowrates. It indicates that without THAM buffer, the pH value of the solution reaches about 9.0 at both flowrates quickly. In this value the urease began to lose its activity quickly, so the urea conversions for unbuffered solution were lower than the buffered urea solution at both flowrates. For buffered urea solutions, the pH value was controlled at about 7.8 for flowrate of 0.06 ml/min and 8.2 for 0.023ml/min. Figure 5.11 also indicates that the higher the flowrate, the lower the urea conversion. For all the cases, the urea conversions decreased as time went by with a power relationship.

The influence of the reactant concentration on the urea conversion is another issue that needs to be addressed. In this study, a six-wave-channel microreactor was used, the urea concentrations at the inlet were 0.1 and 1.0 mol/L, and both were THAM buffered at

pH~7.4. The flowrate of the reactant was 0.023 ml/min. Urease loading for the reactor was 0.01g/gPDMS (66,700 unit/g urease powder). Figure 5.12 shows the urea conversion against time for the two different initial urea solution feeds. The chart indicates that at the initial stage, the reactant with 1.0 mol/L reached higher urea conversion, and its conversion is about 6%, which means 0.06 mol/L urea was converted; at the same time, the reactant with 0.1 mol/L initial concentration had about 0.03 mol/L was converted. After 5~6 hours, both urea conversions dropped to the same level, which is about 0.015 mol/L. It indicated that 1.0 mol/L urea concentration has inhibiting effect on immobilized urease, especially after keeping reactor running for some time. So, although feeding high concentration urea can reach higher urea conversion at the initial stage, using 0.1 mol/L of urea is better in the long run.

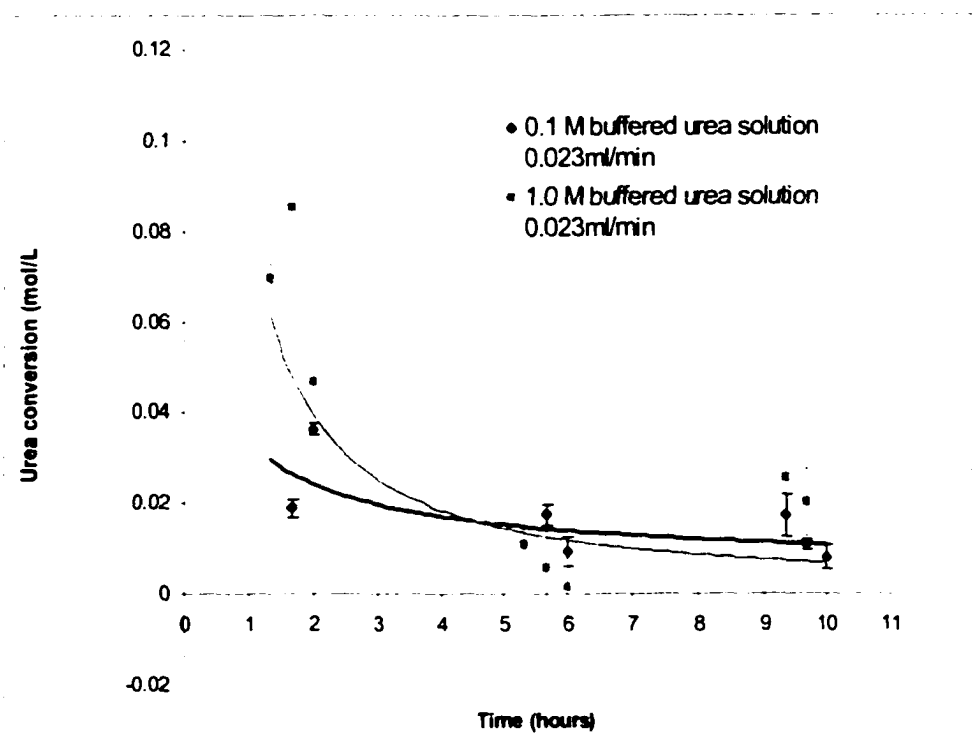

Figure 5.12. Influence of Urea Concentratrion on Reactor Performance

5.3.2 Microreactor Tests with Different Reactor Designs

As described at the previous section, microreactors with different designs were fabricated. The reactors with different designs (straight- and wave-channel) were tested and compared to evaluate the influence of designs on the conversion of urea to carbon dioxide and ammonia. In all cases, the urease loadings of the microreactors were 0.01g/gPDMS. The initial urea concentration at the inlet of the reactors was 0.1 mol/L at pH~7.4. Figure 5.13 shows that the wave-channel reactors highly increased the urea conversion due to its long channel, and wave-structure. The urea conversion for wave-channel reactor was as high as ten almost ten times compared with straight-channel reactor.

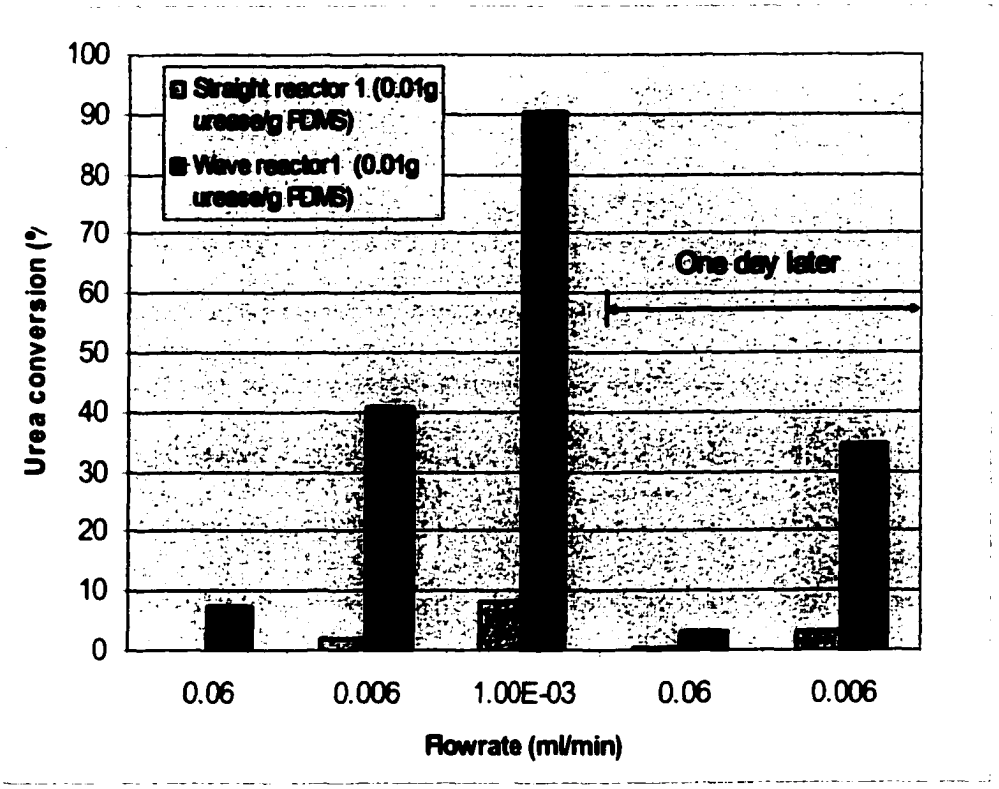

Figure 5.13. Urea Conversion Comparison between Different Reactor Designs

5.3.3 Microreactor Tests with Identical Reactor Designs

To study the influences of operation parameters on the performance of the microreactor, the reactors with identical designs were tested separately. In the study, the straight-channel microreactors with tiny triangle features were evaluated by varying urease loadings (0.01g, 0.02g, 0.03g urease/g PDMS) and flowrates of the urea solution (0.06, 0.006, 0.001 ml/min). The feed urea solution at the inlet was 0.1 mol/L at pH~7.4. The reactors were tested for two days to evaluate the stability of the immobilized urease incorporated in the PDMS polymer. The results are shown in Figure 5.14.

As Figure 5.14 illustrates, for reactors with identical urease loading (0.01g urease/g PDMS), the urea conversion increased as the reactant feeding flowrate dropped. Similar trends were observed in microreactors with 0.02 and 0.03gurease/g PDMS. Figure 5.15 shows the trends of urea conversion changes with the changes of flowrates. It indicates that for all three reactors, the urea conversion increased when the flowrates decreased with a power relationship, which means when the flowrate increased to some extent, and the urea diffusion to the reactive surface became the reaction limiting step on the overall reaction rate. On the other hand, for reactors with different enzyme loadings, the urea conversion increased as the urease loading increased, but the increase is not linear; it slowed down at higher enzyme loadings, and there were large variations of increases at different flowrates. The reason that the increase of urease loadings did not boost the increase of urea conversion so much may lie in the limited reactive surface area in the microchannel. With the low enzyme loading the surface is not saturated with the immobilized urease, but at higher urease loadings, the available active sites for urea

reached maximum due to the surface area limitation, the excessive immobilized urease molecules can not be reached by urea, thus slowed down the urea conversion rate increasing.

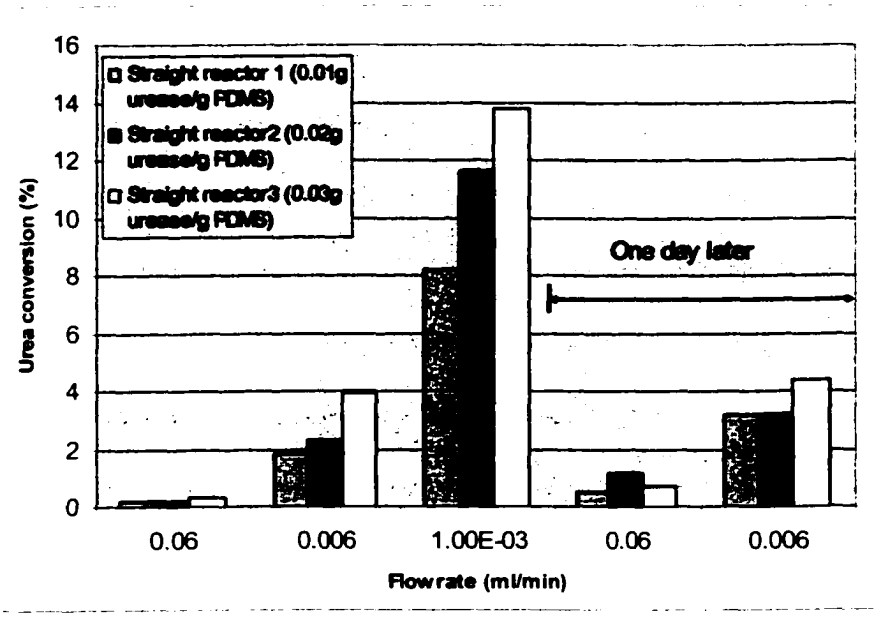

Figure 5.14. Straight-Channel Reactor Tests with Different Enzyme Loadings

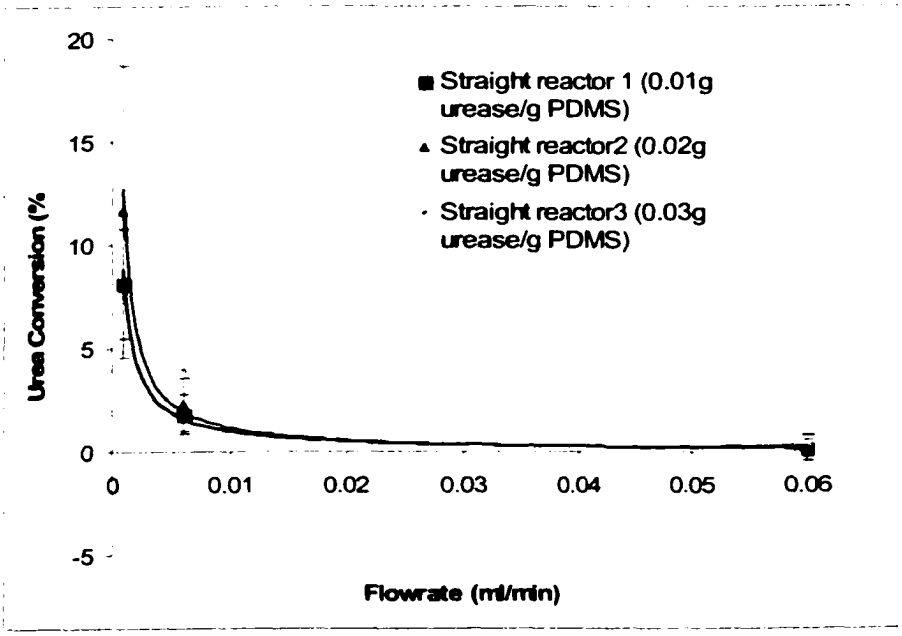

Figure 5.15. Straight-Channel Reactor Tests with Different Flowrates

The microreactors were tested for two days continuously to evaluate the urease activity changes. Figure 5.14 also shows the results of the conversion for two days. Compared the urea conversions at 0.06 ml/min feeding flowrate, it is interesting that, for straight-channel reactors, after one day's running, the urea conversions increased a little for all three reactors, the similar trends were observed for urea conversions with flowrate at 0.006 ml/min.

Figure 5.16 shows the experiment results of single wave-channel reactors with different enzyme loadings and flowrates.

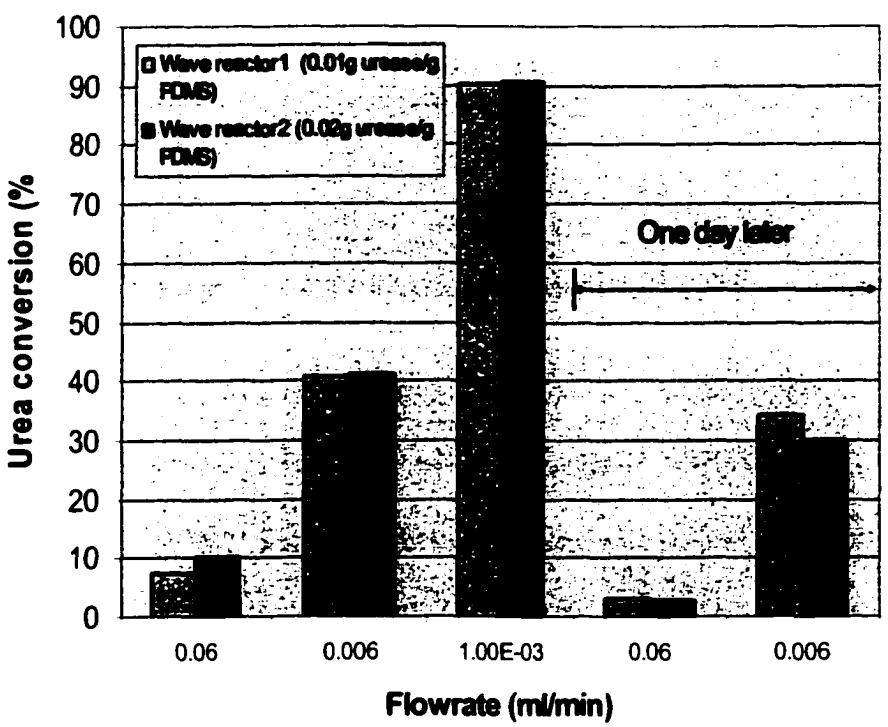

Figure 5.16. Urea Conversions for Single Wave-Channel Reactors

It indicates that increasing the enzyme loading didn't increase the urea conversion rate much; the increases of urea conversion were even much smaller than those for straight-channel reactor. That means that for wave-channel reactors, the high urea

conversion produced higher ammonia concentrations in the microchannels, which significantly inhibited the activities of urease. Thus increasing urease loading would not increase the urea conversion too much. Like the straight-channel reactors, decreasing the feeding flowrates also largely increased the urea conversions.

5.3.4 Wave-Channel Microreactor Tests with Extended Length

The wave-channel microreactors were also tested for extended length. In the study, two wave-channel reactors were connected in a series to double the microchannel length to 100 cm long. From the results of the previous section, the urea conversions for the single wave-channel reactor were still rather low at the flowrates tested. Only at an extremely low flowrate, like 0.001 ml/min, can it reach about 90% conversion. Using the reactors with extended length, the urea conversions may stay high while the flowrates of the urea feedings can increase to a relatively high value.

Figure 5.17 shows the results of urea conversions for single wave-channel reactor and the reactor with extended length (two reactors in a series), and the enzyme loading for both reactors were 0.01g urease/gPDMS. The urea feeding concentration was 0.1 mol/L (THAM buffered at pH~7.4). The reactors were tested for two days with three different flowrates (0.023, 0.048, 0.06 ml/min). The chart shows that the urea conversion for reactor with extended length increased up to four times higher than the single one at flowrate at 0.023 ml/min, three times at 0.048 ml/min, but almost the same at 0.06 ml/min. Still the urea conversion increased when the flowrates decreased following a power relationship.

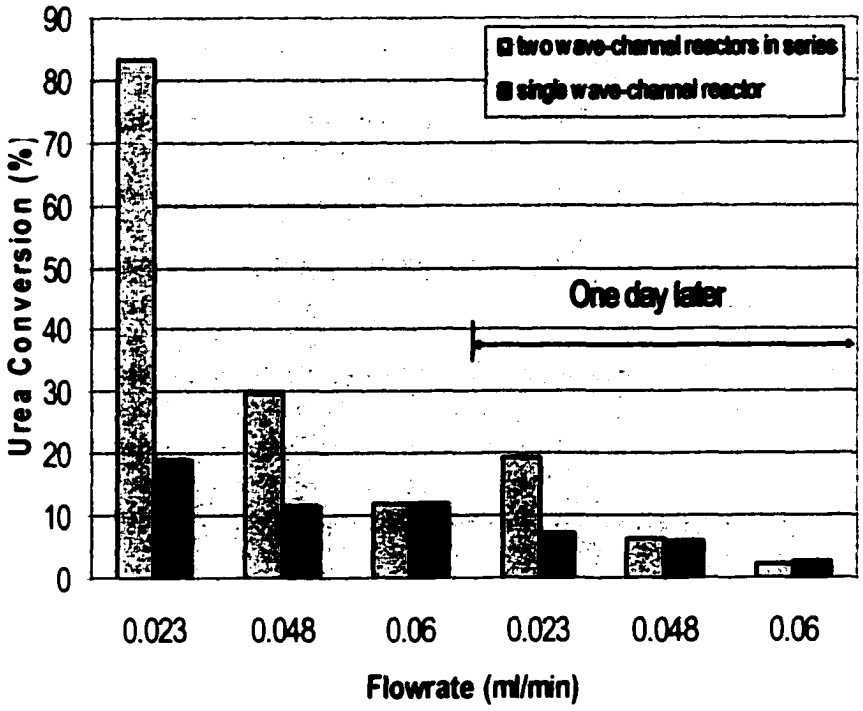

Figure 5.17. Urea Conversions for Single and Two Wave-Channel Reactors

The reactors with extended length were also evaluated by changing urea feeding flowrates and urease loadings. Figure 5.18 shows the results of the experiments. The urea conversion decreased with time in a power relationship. The conversion increased with the increasing of both flowrates and enzyme loadings. For enzyme loading at 0.0327g urease/gPDMS, and the flowrate at 0.023 ml/min, the conversion reached 100% for almost 4 hours before dropping down, and decreased to about 60% conversion after one day's reactor running. For the lowest enzyme loading (0.0113g urease/gPDMS) and highest flowrate (0.073 ml/min), the urea conversion stabilized at about 15% after one day's test. It indicates that for reactors with extended length tested here, much higher flowrate than currently used can be used to achieve high urea conversion. There should be a trade-off between values of flowrate and urease loading.

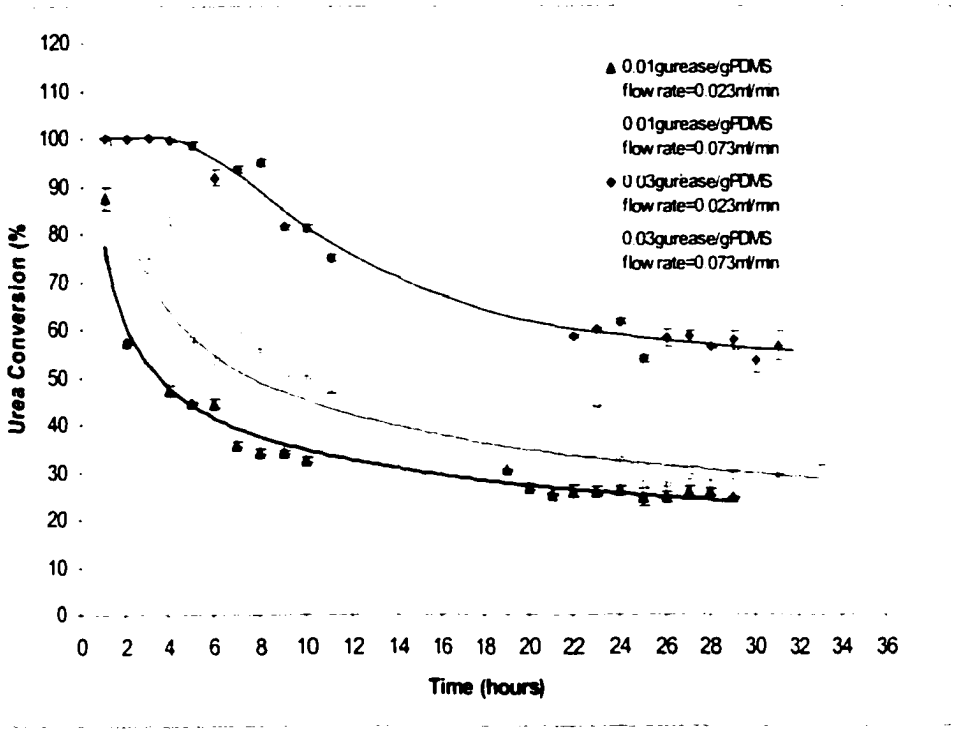

Figure 5.18. Urea Conversions for Wave-Channel Reactors with Extended Length

5.3.5 Enzyme Stability Tests

From the above experiment results shown, all the reactors were tested for two days in order to exam the stability of immobilized urease. Large decreases of urease activities exist in the tests of wave-channel (long-channel) reactors. Decreases of even more than 50% of initial urea activities observed after two days in the experiments. This is a main problem needed to be solved. It may due to the inhibition of ammonia to the urease molecules. For the wave-channel reactors, the ammonia concentration was much higher compared to the straight-channel reactors in the microchannels, which also caused high pH values, those factors seriously inhibit the activity of urease immobilized, and caused immobilized urease lost its activity permanently. High urea conversion need be avoided in order to keep reactor running for a longer time.

5.4 Math Model Simulation Results

In this section the results of the math model simulation for the straight-channel microreactor were presented, the detail of the model was described in the chapter 4, and the expression is as follows:

$$KC_A^2 - [K(C_{AO} - K_M) - a_c A\Delta X V_{max}]C_A - KK_M C_{AO} = 0 \quad \text{.....(5.1)}$$

where $K = V_c A(1 + \frac{C_I}{K_I})$

$$C_I \approx C_{Io} + 2(C_{Ao} - C_A)\Big|_{x+\Delta x}$$

In the simulation, the values of the parameters were used as follows: C_{AO} = 0.1 mol/L in order to neglect the substrate inhibition on the urease activity. The pH value was assumed not to inhibit the activity as swell. The K_M = 4.3×10^{-3} mol/L, and the K_I = 3.3×10^{-3} mol/L were used. The values of the V_{max} were calculated using the experiment results in section 5.2 table 1. The results were showed in table 2 below. The cross section of the channel is 500μm x 200μm =0.1 mm^2, a_c = 0.013587 $\mu m^2/um^3$, calculated using data in Appendix.

Table 5.3. V_{max} Values Related to the Enzyme Loading

	0.25g urease + 50 g PDMS	0.50g urease + 50 g PDMS	1.0g urease + 50 g PDMS
Reaction rate (M/min)	2.0055e-4	7.66914e-4	0.00105
Weight of PDMS beads with urease(g)	10	10	10
Vmax (M/g/min)	2.0055e-5	7.66914e-5	1.05e-4

Note: V_{max} values were taken at urea concentration = 0.1 mol/L according to B. Ramachandran, and D. D. Perlmutter[58].

5.4.1 The Influence of Channel Length on Urea Conversion

The urea conversions were calculated according to three different urease loadings to the PDMS polymer (0.01, 0.02, 0.03 g/g PDMS), and different feeding flowrates: (0.001, 0.006, 0.023, 0.048, 0.06, 0.073 ml/min).

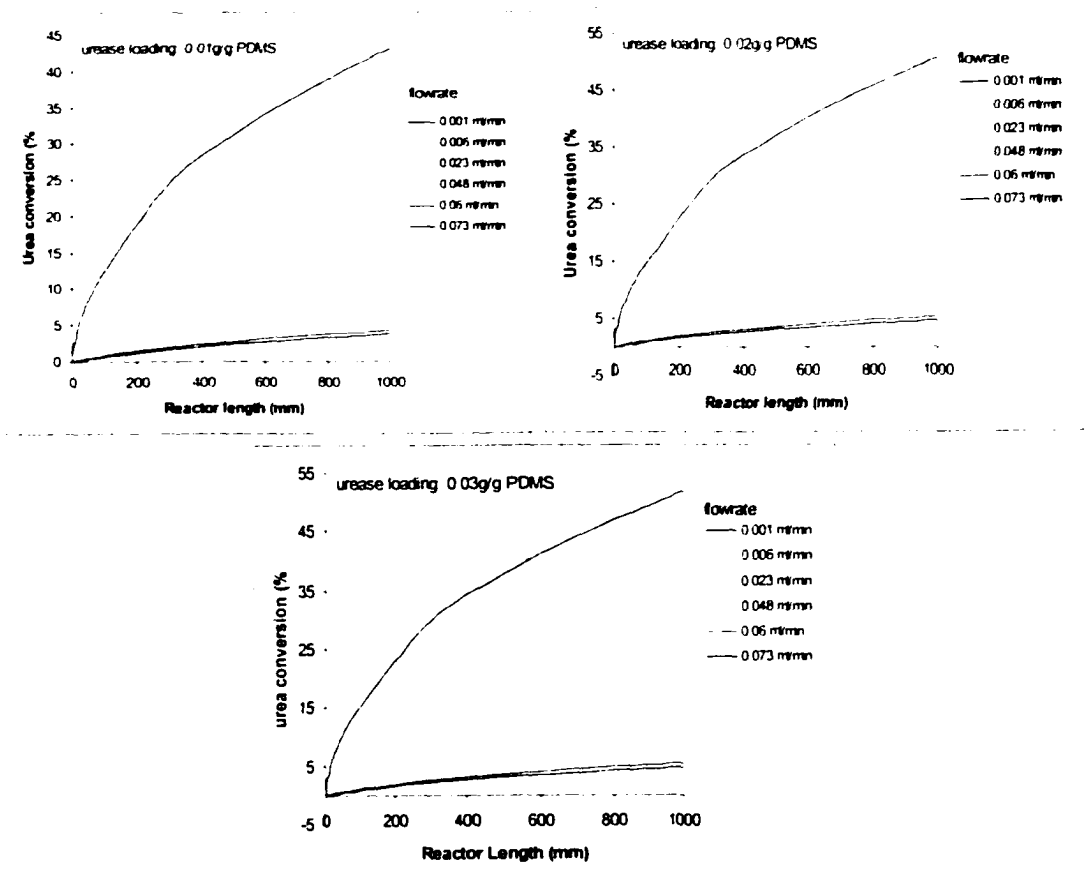

Figure 5.19. Predicted Urea Conversion for Different Channel Lengths

Figure 5.19 shows the simulation results. The urea conversion increased with the increase of channel lengths. With the length increase, the urea conversion rate slowed down. This result is due to the ammonia inhibition on urease activity. The longer the channel length, the more ammonia produced, the more the urease was inhibited, thus slowed down the urea conversion.

5.4.2 The Influence of Flowrates on the Urea Conversion

In this section, the influences of flowrates on urea conversion were calculated. Figure 5.20 showed the predicted results.

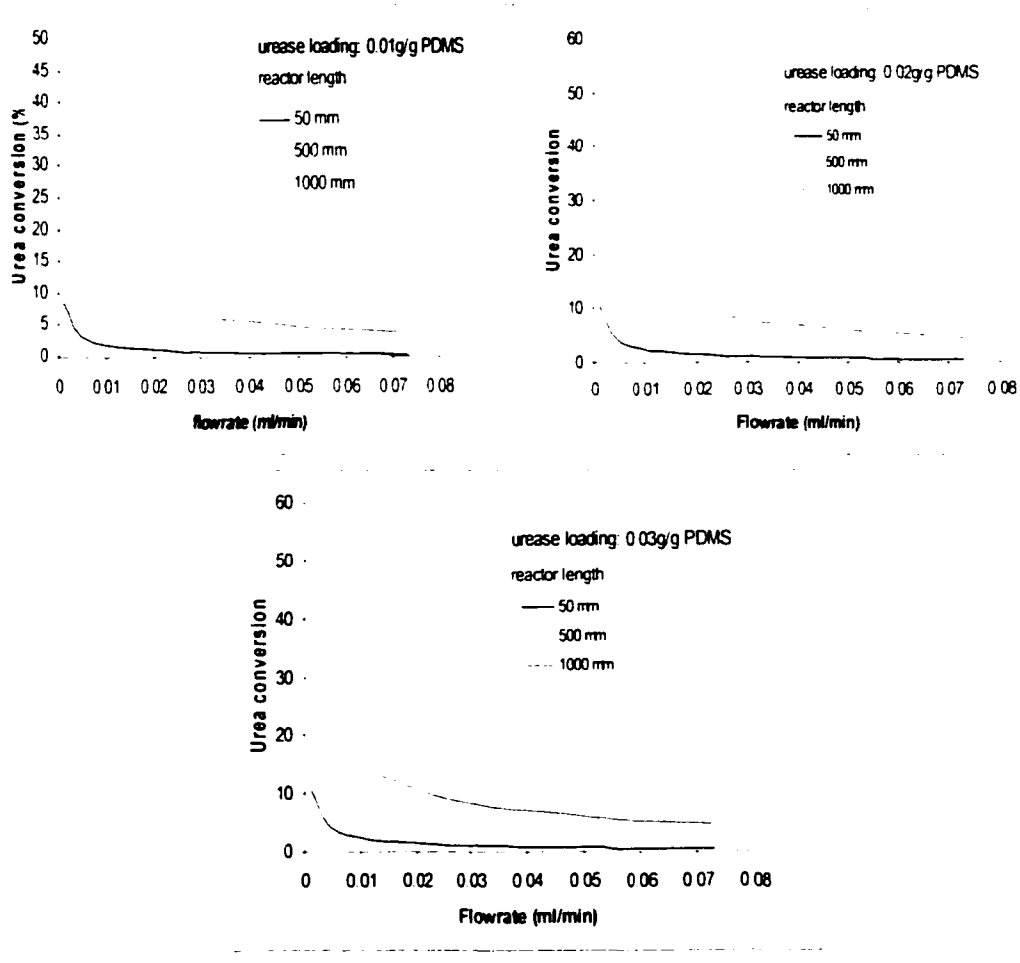

Figure 5.20 Predicted urea conversion fro different feeding flowrates

Three different channel lengths were evaluated individually (50, 500, and 1000 mm), with three enzyme loadings (0.01, 0.02, 0.03 g/g PDMS. The urea conversions were plotted against different flow rates. Figure 5.20 shows that the urea conversion decreased sharply when the flow rate increases from 0 to 0.02 ml/min. and slowed down thereafter. They followed a power relationship, similar to the experiment results.

5.4.3 The Influence of Enzyme Loadings on Urea Conversion

The influences of enzyme loading on the urea conversion were presented in the Figure 5.21. For three different reactor lengths (50, 500, and 1000mm) and all the flowrates evaluated, the urea conversion rate is higher at a lower enzyme loading than that at a higher enzyme loading. These results indicated that with enzyme loading increase, the reactive surface in the microchannels becomes saturated with the immobilized urease, since no extra active sites available to the urea molecules, the urea conversion rate can not increase any more, and reached the maximum value.

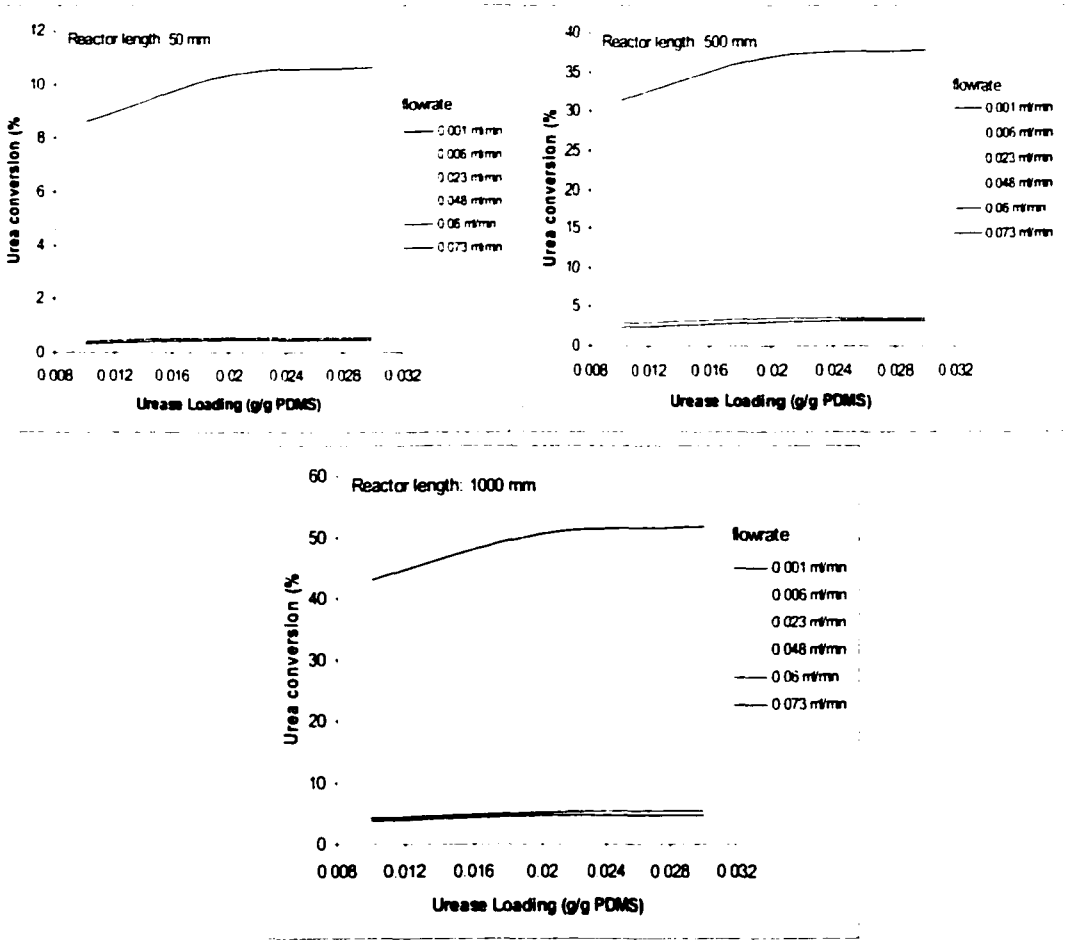

Figure 5.21. Predicted Urea Conversion for Different Enzyme Loadings

5.5 Model Simulation and Experiment Results Comparison

In this section, the math modeling calculation results were compared with the experiments data according to the enzyme loadings, flowrates and the reactor channel lengths. The purpose is to evaluate the extent that the reactor math model can predict the actual microreactor.

Figure 5.22 below shows the comparison results for the straight-channel reactors with channel length of 50 mm. three different enzyme loading (0.01, 0.02, 0.03 g/gPDMs) and three different flowrates (0.06, 0.006, 0.001 ml/min) were used to evaluate the differences between experiment and model predicted results.

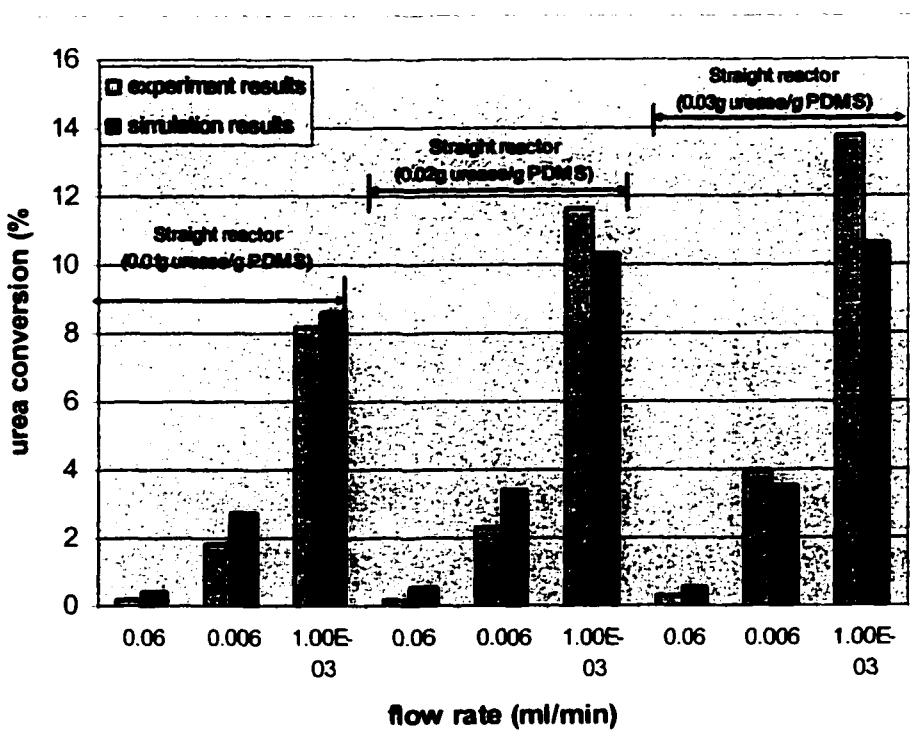

Figure 5.22. Predicted and Experiment Results for Straight-Channel Reactors with Channel Length of 50mm

Figure 5.22 indicates that the model simulation results are consistent with the experiment results for the reactor with 50 mm channel length. At different enzyme

loadings and flowrates, the results of the model are comparable to the experiment results. The maximum deviation is about 20% of the urea conversion. The math model can be applied to predict the performance of an actual straight-channel microreactor with the channel length at this range.

Figure 5.23 shows the model prediction results and the experiment results for the microreactors with channel length of 500 mm for all enzyme loadings and flowrates. Large urea conversion differences are presented in the plot. The urea conversions predicted by the model were much fewer than the experiment results showed. The maximum difference is that the predicted result is less than 70%~80% of the experiment result. For microreactors with channel length of 1000 mm, the urea conversion differences are even much bigger, which is shown in the Figure 5.24 below.

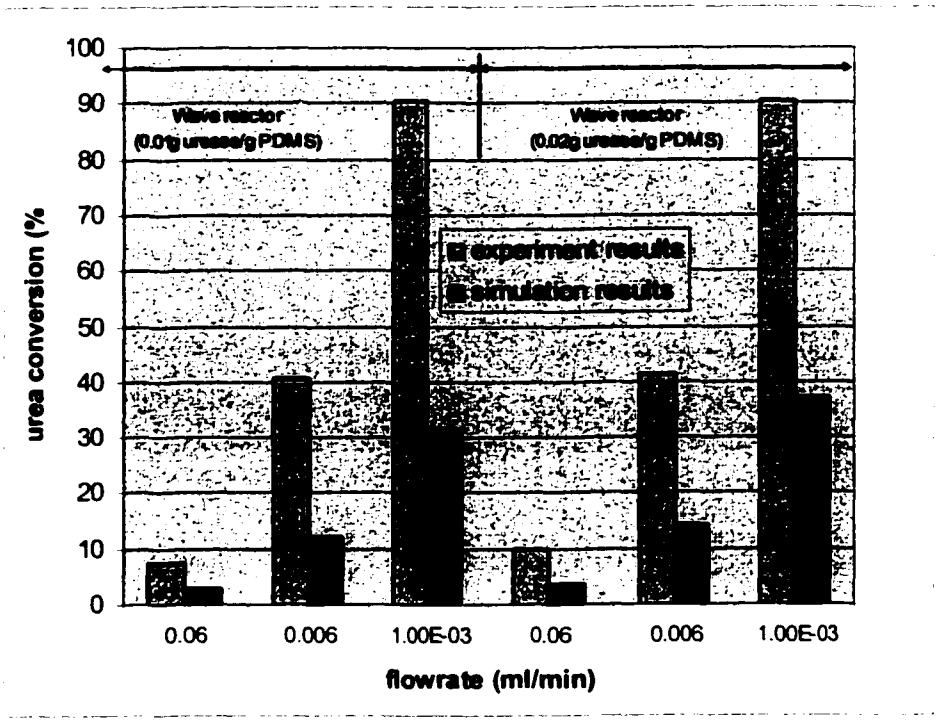

Figure 5.23. Predicted and Experiment Results for Wave-Channel Reactors with Channel Length of 500mm

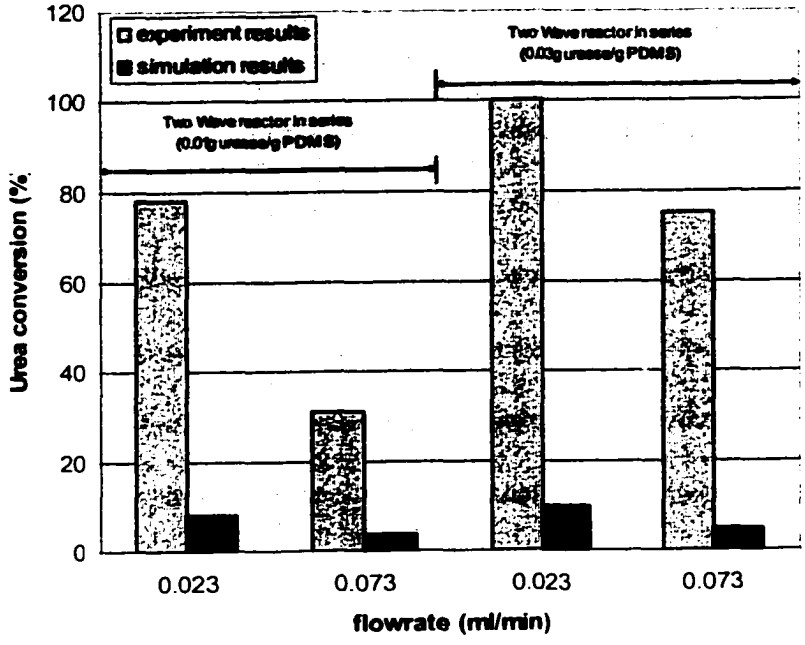

Figure 5.24. Predicted and Experiment Results for Wave-Channel Reactors with Extended Channel Length of 1000mm

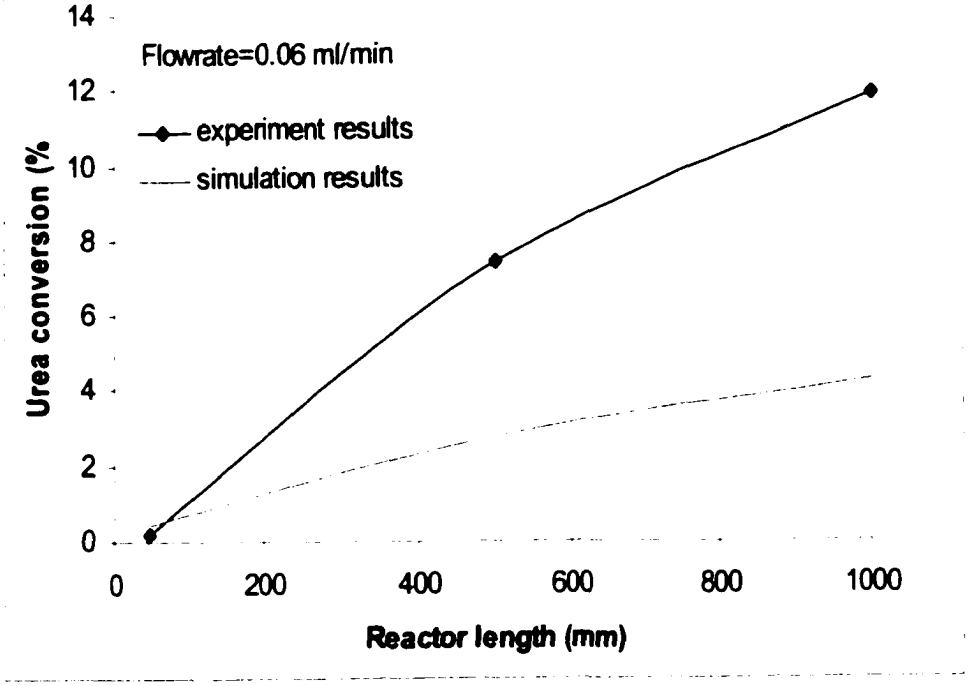

Figure 5.25. Predicted and Experiment Results for Different Channel Length

This tendency is shown more apparently in Figure 5.25. In the plot, the predicted results were compared with the experiment results. The enzyme loading is 0.01g/gPDMs, and the flowrate is 0.06 ml/min.

The reason of the difference is due to the assumptions used in the math model building process. The math model carried a number of assumptions that may have produced large errors when it is used to predict the performance of long-channel microreactors used in the experiments.

The first assumption is that the channels configured in the math model are straight channels. That simplifies the model building process. However, in the experiments, the microreactors with long channels have wave-like channel structures. For both 500mm and 1000mm microreactors, the wave-like channel largely changes types of flow in the channel. It increases average residence time of urea molecules in the channel. The longer residence time means the urea molecules can stay longer in the microchannel, thus increasing the chance for the molecule to reach the reactive surface and react with the immobilized urease.

The second assumption is that in the math model, the reaction is assumed only to be confined on the external reactive surface. No urea diffuses into the internal of the reactive PDMS walls. Actually, the former experiments showed that the PDMS with urease loaded presented the big swelling properties; that is, it easily adsorbed solution with urea into the PDMS networks. This process is controlled by the diffusion process, which is usually the control step for the reaction in the PDMS networks. The reaction inside the producted the ammonia ions and largely increases the local pH value, that inhibit the urease activity inside the PDMS to some extent. But the reaction inside the

PDMS still converted the urea a great deal, and can not be neglected, especially for the long channel microreactors which have the accumulating effect for the urea conversion along the channel. The longer the channel length, the more the conversion difference between predicted and experiment results.

The third assumption is that in the microchannels, all the ammonia molecules are converted to the ammonia ions, so it is largely increased the activity inhibition for the math model. In reality, although most ammonia presented in the solution at pH ~ 7.4 is in the ion form, the ratio of ammonia to ammonium ions is considerable. That means the math model overestimated the inhibition effect of ammonium ions on the urease activity in the PDMS, particularly for the long-channel reactors.

Figure 5.26 shows the results comparison for the influences of urease loadings on the urea conversion. The comparison is conducted on the straight-channel reactors with channel length of 50 mm. Three flowrates were applied (0.001, 0.006, 0.06 ml/min). The plot indicated the differences of the results between predicted and experiment results, especially for the higher enzymes loadings. At higher enzyme loadings, experiment results tended to be higher than the predicted results. The reason seems to be the influence the V_{max} values on the model predictions. V_{max} value characterizes the enzyme activity in the microreactor. The V_{max} values applied in the math models are estimated using batch reactors, which is also used to evaluate the immobilized urease activity in the previous sections. In the batch reactors, the ammonia ions concentrations and the PH values increased with time, which means with time elapsing, the urease activity decreased. So the estimated V_{max} value is smaller than the actual value. For the high enzyme

loadings, the inhibition effects are more serious, so the V_{max} value is smaller. That resulted in the differences of the predicted and experiment results in the microreactors.

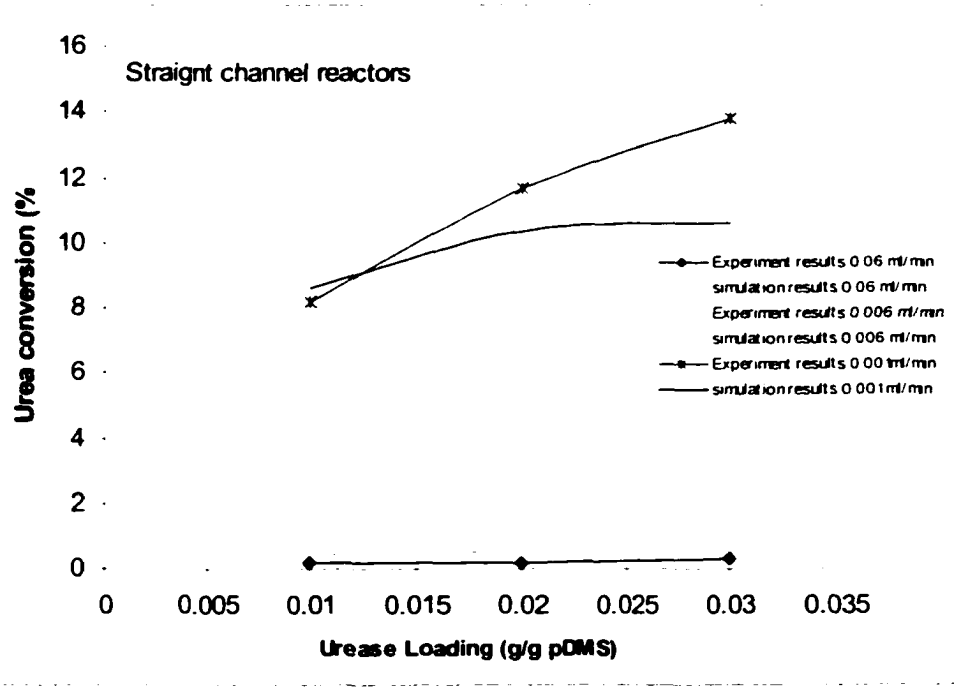

Figure 5.26. Predicted and Experiment Results for Straight-Channel Reactors with Different Enzyme Loadings

CHAPTER VI

CONCLUSION

In this study, bio-micoreactors using a PDMS polymer as a support material have been successfully fabricated. The standard micromanufacturing technology was employed here for the reactor mold generation and resulted in good templates for the easily and microreactor producing. The molds can also be used repeatedly without causing damage. The biocompatible PDMS polymer forms a soft and flexible elastomer exhibiting excellent dielectric, stress-relieving and vibration-absorbing properties over a wide temperature and humidity range. The minimum features generated in the microreactor channel can be reached about 50 um length without significant damage to the channel structure. And on one silicon wafer with diameter of four inches, a microchannel with a length as long as 50 cm. can be fabricated.

Different enzyme immobilization methods on the PDMS polymer were evaluated. One used CMC as crosslinker between enzyme and polymer network; the other method is directly dispersing and incorporating urease powder in the PDMS polymer network after curing process. The urease activities for two different immobilization methods were tested. The urease immobilized using direct incorporating method showed much high activity, and was chosen for the later microreactor evaluations. Different enzyme loadings were evaluated, and the immobilized urease maintaining as much as 70% of its

original values after 30 days was achieved. Though the variation of urease activity is big, and need to be studied further.

Different reactor designs (straight- and wave-channels) were evaluated, which provided significant insight to the bio-polymer microreactors. Small triangle features were designed in the channels to increase the reactive surface area, and also served a reactant mixer. The evaluation results showed that the pH buffer solution (THAM) can stabilize the pH value in the reactor and prevent the urease from activity decrease. The lower urea concentration is necessary in order to neglect the substrate inhibition on the urease activity. In the study, although the straight-channel microreactors can provide the urea conversion as much as 14% percent at very low flowrate, the urea conversion in the wave-channel microreactor can easily reach higher values at much higher flowrate. The urea conversions as high as 90% were reached. And if two wave-channel reactors connected together in a series, 100% urea conversion can be reached at high flowrate without any problem. But the urease stability is a big problem in the wave-channel reactors, due to the ammonia and pH inhibition, the immobilized urease quickly lost its activity quickly in wave-channel reactors. There should be a trade-off between these two factors. On the other hand, since increasing channel length can greatly boost the urea conversion by increase the reactive surface area, the microchannel may be scaled down further to increase the surface area to volume ratio, thus can achieve higher urea conversion for the same reactor size.

A mathematical model was employed here to compare with the experiment results and served for predicting the urea conversion in the PDMS microreactors. The results indicated that the predicted results are consistent with the experiment results for the

straight-channel reactors with channel of 50 mm, but for the wave-channel reactors, there are large deviations. The longer the channel length, the bigger the difference. The reason is that the math modeling has several assumptions which affect the final results for longer channel reactors. First, the reaction happened not only on the reactive surface, but only inside the PDMS networks. Second, the model assumed straight channels, but the wave-channel largely changed the fluid dynamic characteristics in the microreactor channels, the wave channel increased the reactant residence time in the reactor, thus increased the urea conversion. Third, the model assumed all the ammonia molecules are in the ionic forms, but in reality not all ammonia molecules under the testing conditions are in the ionic forms. The model overestimated the inhibition of ammonium ions on the urease activities.

In future work, a new or modified mathematical model needs to be developed for the microreactor with wave-channels. The urea-urease hydrolysis is necessary to be taken into account to predict the urea conversion more accurately.

Along with the model problems, there are some other problems need to be addressed. The first one is about the reactor system assembly issues. Although the PDMS is self-sealed to most materials surface such as glass, plastics, and etc, the reactor channel sealing still a big problem. Because the microscale of the reactor channels, even the small flowrate can cause big pressure drops along the microchannels, thus causing high stresses on the edge of the channel. It is difficult to seal to microreactor channels with distort the channel structure, and results in either leakage or channel blocking problems, and resulted in big variations in test results. New reactor sealing method need to be explored.

The second one is the enzyme immobilization technology, although the direct incorporating methods provided high urease activities. It consumed a large amount of urease during the immobilization process; in other words, the utilization of urease is not efficient. Thus further efforts for improving this method or exploring new enzyme immobilization techniques on the PDMS polymer are recommended.

APPENDIX

SURFACE AREA AND VOLUME FOR WAVE-CHANNEL REACTOR

APPENDIX

Table A1. Net Reactive Surface Area of the Wave-channel Microreactor

Surface area for single HALF RING part of channel bottom	$(875^2 - 375^2)\ \pi/2 = 981718.75\ um^2$
Surface area for single HALF RING walls	$(875 + 375) \times \pi \times 200 = 785375\ um^2$
Surface area for single triangle feature bottom	$140 \times 125/2 = 8750\ um^2$
Surface area for single triangle feature walls	$(143+143+140) \times 200 = 85200\ um^2$
Surface area for single sub-straight channel bottom	$10500 \times 500 - 8750 \times 21 \times 3 = 4698750\ um^2$
Surface area for single sub-straight channel walls	$10500 \times 200 \times 2 = 4200000\ um^2$
Total surface area for single sub-straight channel with triangle features	$4698750 + 4200000 + 85200 \times 21 \times 3 = 14266350\ um^2$
Total surface area for single zigzag channel with triangle features	$14266350 \times 40 + (981718.75 + 785375) \times 40 = 641337750\ um^2 = 641.33775\ mm^2$
Total surface area for whole reactor (six channels)	$641.33775 \times 6 = 3848.0265\ mm^2$

Table A2. Net Volume of the Wave-channel Microreactor

Volume for single HALF RING part of channel	$981718.75 \times 200 = 196343750\ um^3$
Volume for single triangle feature	$8750 \times 200 = 1750000\ um^3$
Volume for single sub-straight channel with triangle features	$10500 \times 500 \times 200 - 1750000 \times 21 \times 3 = 939750000\ um^3$
Total volume for single zigzag channel with triangle features	$(939750000 + 196343750) \times 40 = 45443750000\ um^3 = 45.44375\ mm^3$
Total volume for whole reactor (six channels)	$45.44375 \times 6 = 272.6625\ mm^3$

REFERENCES

1. Ravi Srinivasan, I-Ming Hsing, Peter E. Berger, Klavs F. Jensen, etc. "*Micromachined Reactors for Catalytic Partial Oxidation Reactions*". ALChE Journal, November 1997, Vol. 43, No.11.

2. Robert S. Wegeng, Charles J. Call, and M. Kevin Drost. "*Chemical System Miniaturization*". Pacific Northwest National Laboratory, PNNL-SA-27317.

3. Dean W. Matson, Peter M. Martin, Donald C. Stewart. "*Fabrication of Microchannel Chemical Reactors Using a Metal Lamination Process*". 1999 Battelle, PNNL.

4. Saliha Bacha, Marielle Montagne, and Alain Bergel. "*Modeling Mass Transfer with Enzymatic Reaction in Electrichemical Multilayer Microreactors*". AIChE Journal, October 1996, Vol. 42, No. 10.

5. A. Folch, A. Ayon, O. Hurtado, M. A. Schmidt, M. Toner. "*Modeling of Deep Polydimethylsilixane Microstructures for Microfluidics and Biological Applications*". Journal of biomechanical Engineering, Feburary 1999 Vol. 121.

6. R. Scott Martin, Andrew J. Gawron, and Susan M. Lunte. "*Dual-Electrode Electrochemical Detection for Poly(dimethylsiloxane)-Fabricated Capillary Electrophoresis Microchips*". Analytical Chemistry, Vol. 72, No. 14, July 15 2000.

7. David, C. Duffy, J. Cooper Mcdonald, Olivier J. A. Schueller, etc. "*Rapid Prototyping of Microfluidic Systems in Poly(dimethylsiloxane)*". Analytical Chemistry, 1998, 70, 4974-4978.

8. Jin Sung Yoo, Sung Jun Kim, and Joong So Choi. "*Swelling Equilibria of Mixed Solvent/Poly(dimethylsiloxane) Systems*", 1999, American Chemical Society. Published on Web 11/14/1998.

9. Hidetoshi Oikawa and Kenkichi Murakami. "*Some Comments on the Swelling Mechanism of Rubber Vulcanizates*". Rubber Chemistry and Technology vol.60. 1986.

10. AntonioN. Falcao, Jan Skov Pedersen, and Kell Mortensen. "*Polydimethylsiloxane Networks at Equilibrium Swekking: Extracted and Nonextracted Networks*". Macromolecules 1996, 29, 809-818.

11. A. G. Andreopoulos, G. L. Polyzois, and M. Evangelaton. "*Swelling Properties of Cross-linked Maxillofacial Elastomers*". Journal of Applied Polymer Science, vol. 50, 729-733 (1993).

12. Yanqun Zhao and B. E. Eichinger. "*Study of Solvent Effects on the Dilation Modulus of Poly(diemthylsiloxane)*". Macromolecules 1992, 25, 6988-6995.

13. L. Z. Rogovina, V.G. Vasil'ev, and G. L. Slonimskii. "*Influence of the Nature and Concentration of the Solvent on the Formation and Properties of Polydimethylsiloxane Networks*". Polymer Science USSR, vol. 32, No. 10, pp1997-2004, 1990.

14. C. J. Guo and D. De Kee. "*Effect of Molecular Structure on Diffusion of Organic Solvents in Rubbers*". Chemical Engineering Science, vol. 47, no. 7, pp 1525-1532, 1992.

15. Ping Wang, Jerry H. Meldon, and Nakho Sung. "*Heat Effects in Sorption of Organic Vapors in Rubbery Polymers*". Journal of Applied Polymer Science, vol. 59, 937-944 (1996).

16. Blume, P. J. F. Schwering, M. H. V. Mulder and C. A. Smolders. "*Vapour Sorption and Permeation Properties of Poly(dimethylsiloxane) Films*". Journal of Membrane Science, 61 (1991) 85-97.

17. M. B. Davydova, Yu P. Yampol'skii, and S. G. Durgar'yan. "*Sorption of Hydrocarbons in Polyvinyltrimethylsilane and Polydimethyl Siloxane with Nickel Acetylacetonate Additives*". Polymer Science USSR, vol. 30, no. 7 pp 1501-1507, 1988.

18. Erik Baltussen, Frank David, Pat Sandra, and etc. "*Equilibrium Sorptive Enrichment on Poly(dimethylsiloxane) Particles for Trace Analysis of Volatile Compounds in Gaseous Samples*". Analytical Chemistry, 1999, 71, 5193-5198.

19. V. M. Shah, B. J. Hardy, and S. A. Stern. "*Solubility of Carbon Dioxide, Methane, and Propane in Silicone Polymers: Effect of Polymer Side Chains*" Journal of Polymer Science: Part B: Polymer Physics, vol. 24, 2033-2047 (1986).

20. B. Lendl, R. Schindler, J. Frank, and R. Kellner. "*Fourier Transform Infrared Detection in Miniaturized Total Analysis Systems for Sucrose Analysis*" Analytical Chemistry 1997, 69, 2877-2881.

21. Geza Nagy, Clarke X. Xu, Richard P. Buck, etc. "*Wet and Dry Chemistry Kits for Total Creatine Kinase Activity using a Microfabricated, Planar, Small-volume, Amperometric Cell*". Analytica Chemica Acta 377 (1998) 1-12.

22. Fernando J. Beltran, Juan F. Garcia-Araya, and Pedro M. Alvarez. "*Integration of Continuous Biological and Chemical (ozone) Treatment of Domestic Wastwater:1. Biodegradation and Postozonation*". Journal of Chemical Technology and Biotechnology. 74:877-883 (1999).

23. Larry Licklider, Werner G. Kuhr, Martin P. Lacey, etc. "*On-line Microreactors/Capillary Electrophoresis/Mass Spectrometry for the Analysis of Proteins and Peptides*". Analytical Chemistry, vol. 67, no. 22, 1995.

24. Masahiro Goto, Masaki Miyata, Noriho Kamiya, and Fumiyuki Nakashio. "*Novel Surfactant-coated Enzymes Immobilized in Poly(ethylene Glycol) Microcapsules*". Biotechnology, volume 9 no. 2 (feburary, 1995) pp. 81-84.

25. Yoshitsune Shin-ya, Toshio Kajiuchi. "*Chitosan Hydrolysis Using Chitosanolytic Enzymes Modified With Polyalkyleneoxide-Maleic Anhydride Copolymer*". Journal of Chemical Engineering of Japan, vol. 31, no. 6 pp 930-935, 1998.

26. Michal Bodzek, Jolanta Bohdziewicz, and Malgorzata kowalska. '*Preparation of Membrane-Immobilized Enzymes for Phenol Decomposition*". J. of Chem. Tech. Biotechnol. 1994, 61, 231-239.

27. F. Camacho-rubio, E. Jurado-Alameda, P. Gonzalez-tello, and G. Luzon Gonzalez. "*A Comparative Study of the Activity of Free and Immobilized Enzymes and Its Application to Clucose Isoerase*". Chemical Engineering Science, vol. 51 no. 17, pp 4159-4165, 1996.

28. Kakamitsu Lida, Daisuke Maruyama, and Kimitoshi Fukunaga. "*Stabilization of Entrapped Catalase using Photo-corsslinked Resin Gel for Use in Wastewater Containing Hydrogen Peroxide*". Journal of. Chemical Technology and Biotechnology, 75: 1026-1030 (2000).

29. David A. Glassner and Eric A. Grulke. "*Characterization of an Immobilized Biocatalyst System for Production of Thermostable Amylase*". Biotechnology Process (vol. 5 no. 1), March, 1989.

30. Kakeshi Gotoh and Ken-ichi Kikuchi. "*Immobilization of Biological Membrane by Sonication and Freeze-Thawing*". Journal of Chemical Engineering of Japan, Vol. 31, no. 5, pp 860-863, 1998.

31. M. D. Luque de Castro, Rafael Quiles, etc. "*Continuous-flow Assay with Immobilized Enzymes for Determining of Inorganic Phosphate in Serum*". Clin. Chem. 41/1, 99/102, 1995.

32. Kodansha Ltd, and Hohn Wiley & Sons. "*Immobiloized Enzymes: Research and Development*". A Halsted Press Book, 1978. ISBN 0-470-26531-0.

33. H. Jean Wang, Ronald L. Thomas, etc. "*Enzymes Immobilized On Formed-in-Place Membranes for Food Processing: Procedures and Properties*". Journal of Food Process Engineering, 17 (1994) 365-381.

34. I. Ming Hsing, Pavi Srinivasan, Michael P. Harold, etc. "*Simulation of Micromachined Chemical Reactors for Heterogeneous Partial Oxidation Reactions*", Chemical Engineering Science 55 (2000) 3-13.

35. Gisella M. Zanin and Flavio F. De Moraes. "*Thermal Stability and Energy of Deactivation of Free and Immobilized Amyloglucosidase in the Saccharification of Liquefied Cassava starch*". Applied Biochemistry and Biotechnoology, vol. 70-72, 1998.

36. Joseph Wang, Jie liu, and Gemma Cepra. "*Thermal Stabilization of Enzymes Immobilized within Carbon Paste Electrodes*". Analytical Chemistry, 1997, 69, 3124-3127.

37. Maria A. Longo, and Didier Combes. "*Thermostability of Modified Enzymes: a Detailed Study*". Journal of. Chemical Technology and Biotechnology, 74: 25-32, 1999.

38. Stephen B. Lamb, and David C. Stuckey. "*Factors Influencing the Stability of a Novel Enzyme Immobilization Support-Colloidal Liquid Aphrons (CLAs)*". Journal of. Chemical Technology and Biotechnology, 75: 681-688 (2000).

39. Felix J. B. Kremer, Johan F. J. Engbersen, Jans Kruise, etc. "*Immobilization and Activity of Concanavalin A on Tantalum Pentoxide and Silicon Dioxide Surfaces*". Sensors and Actuators B, 13-14 (1993) 176-179.

40. Leonard J. Schussel and James E. Atwater. "*A Continuous Alcohol Oxidase Bioreactor for Regenerative Life Support*". Enzyme and Microbial Technology 18: 229-235, 1996.

41. Isabella Moser, Thomas Schalkhammer, Eva Mann-Buxbaum, and Gernard Hawa. "Advanced Immobilization and Protein Techniques on Thin Film Biosensors". Sensors and Actuators B. 7 (1992) 356-362.

42. Simon Ekstrom, Patrik Onnerfjord, Johan Nilsson, etc. "*Integrated Microanalytical Technology Enabling Rapid and Automated Protein Identification*". Analytical Chemistry, 2000, 72, 286-293.

43. Jiang Bo and Xiang Ming. "*Immobilization of Enzymes on Polymers Modified by Ultrasonic Irradiation*". Eur. Polym. J. vol.28, no. 7, pp 827-830, 1992.

44. JMS Rocha, MH Gil, and FAP Garcia. "*Optimization of the Enzymatic Synthesis of N-octyl Oleate with Immobilized Lipase in the Absence of Solvents*". Journal of Chemical Technology and Biotechnology, 74: 607-612 (1999).

45. Anna Wojcik, Jerzy Lobarzewski, and Teresa Blaszczynska. "*Immobilization of Enzymes to Porous-bead Polymers and Silica Gel Activated by Graft Polymerization of 2,3-Epoxypropyl Methacrylate*". Journal of Chemical Technology and Biotechnology, 48: 287-302, (1990).

46. R. A. Williams and H. W. Blanch. "*Covalent Immobilization of Protein Monolayers for Biosensor Applications*". Biosensors & Bioelectronics 9 (1994) 159-167.

47. Ping Wang, Maria V. Sergeeva, Lilian Lim, and Jonathan S. Dordick. "*Biocatalytic Plastics as Active and Stable Materials for Biotransformations*". Nature Biotechnology, volume 15, August 1997.

48. I. A. Kravchenko, T. I. Davidenko, and R. I. Chalanova. "*Study of Proteolytic Enzymes Immobilized on Hydrophilic Polymers*". Pharmaceutical Chemistry Journal vol. 32, no. 5, 1998.

49. Robert F. Service. "Chemists *Clean Ceramics and Coat Enzymes in Plastic*". Science, vol. 272, 12 April 1996.

50. Zhen Yang, Anita J. Mesiano, etc. "*Activity and Stability of Enzyme Incorporated into Acrylic Polymers*". Journal of American Chemical Society, 1995, 117, 4843-4850.

51. Ping Wang, and Jonathan S. Dordick. "*Enzymatic Synthesis of Unique Thymidine-Containing Polyphenols*". Macromolecules 1998, 31, 941-943.

52. Ping Wang, Sudath Amarasinghe, Johna Leddy, Mark Arnold, and Jonathan S. Dordick. "*Enzymatically Prepared Poly(hydroquinone) as a Mediator for Amperometric Glucose Sensors*". Polymer Vol. 39, no. 1 1998.

53. Jean-Pierre, Cohen-Addad. "*Approach to the swelling Characterization of Silica-filled Siloxane Systems*". Polymer Repoerts. October 1986.

54. Paul D Boyer. "*The Enzymes, Volume IV, Hydrolysis, third Edition*". Academic Press, New York and London. 1971".

55. Leonard J. Schussel and James E. Atwater. "*A Urease Bioreactor for Water Reclamation Aboard Manned Apacecraft*". Chemosphere, Vol. 30, no. 5, pp 985-994, 1995.

56. Severian Dumitriu, Marcel Popa, Vlad Artenie, and Florin Dan. "*Bioactive Polymers. 56: Urease Immobilized on Carboxymethylcellulose*". Biotechnology and Bioengineering, Vol. 34, pp 283-290 (1989).

57. Yuri Lvov, and Frank Caruso. "*Ordered Urease/Polyion Shells on Latex Cores: Fabrication and Enzymatic Activity*". To be submitted in J. Colloid and Interface Sci.

58. K. B. Ramachandran, and D. D. Perlmutter. "*Effects of Immobilization on the Kinetics of Enzyme-Catalyzed Reactions. II. Urease in a Packed-Column Differential Reactor System*". Biotechnology and Bioengineering, Vol. XVIII, pp 685-699 (1976).

59. K. J. Laidler, and J. P. Hoare. "*The Molecular Kinetics of the Urea-Urease System. I. The Kinetic Laws*" Journal of American Chemical Society, August, 1949.

60. K. J. Laidler, and J. P. Hoare. "*The Molecular Kinetics of the Urea-Urease System. II. The inhibition by Products*" Journal of American Chemical Society, June, 1950.

61. K. J. Laidler, and J. P. Hoare. "*The Molecular Kinetics of the Urea-Urease System. III. Heats and Entropies of Complex Formation and Reaction*" Journal of American Chemical Society, June, 1950.

62. Robert L. Blakeley, John A. Hinds, Hugo E. Kunze, etc. "*Jack Bean Urease (EC 3.5.1.5). Demonstration of a Carbamoyl-Transfer Reaction and Inhibition by Hydroxamic Acids*". Biochemistry, vol. 8, no. 5 May 1969.

63. Kent M. Harmon, and Carl Niemann. "*The Competitive Inhibition of the Urease-Catalyzed Hydrolysis of Urea by Phosphate*". The Journal of Biological Chemistry, Vol. 177, 1949.

64. James B. Summer, David B Hand, and Rachel G. Holloway. "*Studies of the Intermediate Products Formed During the Hydrolysis of Urea by Urease*". January, 1931.

65. H. J. Moynihan, C. K. Lee, W. Clark, and N. H. L. Wang. "*Urea Hydrolysis by Immobilized Urease in Fixed-bed Reactor: Analysis and Kinetic Parameter Estimation*". Biotechnology and Bioengineering, Vol 34, pp 951-963 (1989).

66. P. T. vasudevan, L. Ruggiano, and R. H. Welland. "*Studies on the Deactivation of Immobilized Urease*". Biotechnology and Bioengineering, Vol 35, pp 1145-1149, (1990).

67. S. Paddeu, A. Fanigliulo, M. Lanzi, T. Dubrovsky, and C. Nicolini. "*LB-based PAB Immunosystem: Activity of an Immobilized Urease Monolayer*". Sensors and Actuators B 24-25 (1995) 976-882.

68. Cynthia K. Dickey. "*The Design, Modeling, Fabrication, and Testing of an Immobilized Enzyme Microreactor*". A Dissertation for Doctor Philosophy in Biomedical Engineering, Louisiana Tech University, 2000.

69. Qing Deng, "*A Study on Simulation and Fabrication of a Microreaction Device*". A thesis For Master of Science, Louisiana Tech University, 2000.

70. Zhixuan Zhu, "*A Study on Layer-by-Layer Assembly of Urease and Polyions*". A Thesis for Master of Science, Louisiana Tech University, 2001.

71. "*Separation and Determination of Allantoin, Uric Acid, Hydantoin, and Urea*". Journal of Chromatography-A. 4 Nov. 1994, 684(2):350-353.

72. "*Determination of Urea and Its Thermal Decomposition Products by High-Performance Liquid Chromatography*". Journal of Chromatography-A. 6 Jan. 1995, 689(1):164-169.

73. "*Solid-Phase Extraction (SPE) of Blood Urea Compared with Liquid-Liquid Extraction Regarding Artifact Formation*". Journal of Liquid Chromatography. Jun 1995, 18(11): 2167-2174.

74. "*Information About High Technology Silicone Materials, Sylgard 184 Silicone Elastomer, Base & Curing Agent Data Sheet*". Dow Corning Corporation, 1991.

75. "*Nano SU-8 Resists: Negative UV sensitive Resists for MEMS/Microsystem Applications*". MicroChem Corporation, March, 1998.

76. Humphery Joseph Moynihan. "*Reaction and Mass Transport in Immobilized Urease Reactions: Simulation and PH control*". A Dissertation fro the Degree of Doctor of Philisophy, Purdue University, 1987.

77. W. Ehrfeld. "*Implementation of Microreaction Technology in Process Engineering and Biochemistry*", 3rd International Conference on Microreaction Technology, April, 1999.

78. H. M. Chandler, J. C. Cox, K. Healey, etc. "*An Investigation of the Use of Urease-Antibody Conjugates in Enzyme Immunoassays*". Journal of Immunological Methods, 53, (1982), 187-194.

79. H. Scott Fogler. "Elements of *Chemical Reaction Engineering*". 3rd Edition, Prentice Hall PTR, 2001, ISBN 0-13-531708-8.

80. R. B. Bird, W. E. Stewart, and E. N. Lightfoot. "*Transport Phenomena*". John Wiley & Sons, 1960. ISBN 0-471-07392-X.

81. Marc Madou. "Fundamentals of Microfabrication". CRC Press, ISBN 0-8493-9451-1.

82. L. Goldstein and E. Katchalski-Katzir. "Immobilized Enzymes- A Survey". Applied Biochemistry and bioengineering, vol. 1, p 127, 1976.

83. M. Dixon, and E. C. Webb. "Enzymes". Academic Press, New York, 1964.